

Energy transfer of excitons between quantum wells separated by a wide barrier

S. K. Lyo

Sandia National Laboratories, Albuquerque, New Mexico 87185

(Received 22 December 1999; revised manuscript received 11 April 2000)

We present a microscopic theory of the excitonic Stokes and anti-Stokes energy-transfer mechanisms between two widely separated unequal quantum wells with a large energy mismatch (Δ) at low temperatures (T). Several important intrinsic energy-transfer mechanisms have been examined, including dipolar coupling, real and virtual photon-exchange coupling, and over-barrier ionization of the excitons via exciton-exciton Auger processes. The transfer rate is calculated as a function of T and the center-to-center distance d between the wells. The rates depend sensitively on T for plane-wave excitons. For localized excitons, the rates depend on T only through the T dependence of the exciton localization radius. For Stokes energy transfer, the dominant energy transfer occurs through a photon-exchange interaction, which enables the excitons from the higher-energy wells to decay into free electrons and holes in the lower-energy wells. The rate has a slow dependence on d , yielding reasonable agreement with recent data from GaAs/Al_xGa_{1-x}As quantum wells. The dipolar rate is about an order of magnitude smaller for large d (e.g., $d = 175 \text{ \AA}$) with a stronger range dependence proportional to d^{-4} . However, the latter can be comparable to the radiative rate for small d (e.g., $d \leq 80 \text{ \AA}$). For anti-Stokes transfer through exchange-type (e.g., dipolar and photon-exchange) interactions, we show that thermal activation proportional to $\exp(-\Delta/k_B T)$ is essential for the transfer, contradicting a recent nonactivated result based on the Förster-Dexter's spectral-overlap theory. Phonon-assisted transfer yields a negligibly small rate. On the other hand, energy transfer through over-barrier ionization of excitons via Auger processes yields a significantly larger nonactivated rate which is independent of d . The result is compared with recent data.

I. INTRODUCTION

Energy transfer of excitons between deep semiconductor quantum wells and quantum dots separated by thick barriers is not only an academically interesting phenomenon but plays a fundamental role in optoelectronic devices based on artificially structured semiconductors, such as quantum-well (QW) and quantum-dot lasers and light-emitting diodes. While energy transfer inside a single QW has been extensively studied in the past,^{1,2} interwell energy transfer has received considerably less attention. Recently, surprisingly large low-temperature (T) Stokes and anti-Stokes energy-transfer rates have been observed by Tomita, Shah, and Knox³ (TSK) and Kim *et al.*⁴ between two widely separated GaAs/Al_xGa_{1-x}As QW's using time-resolved photoluminescence excitation (PLE) and photoluminescence (PL) spectroscopy. For Stokes transfer, the observed transfer rate from a 50- \AA QW to a 100- \AA QW with an energy mismatch $\Delta = 60 \text{ meV}$ was in the range $3 \times 10^8 - 1 \times 10^9 \text{ sec}^{-1}$ for samples with a center-to-center distance d of 175–375 \AA and at $T = 4 - 80 \text{ K}$. Anti-Stokes transfer from a wide to a narrow QW proceeded at a much slower rate ($10^4 - 10^6 \text{ sec}^{-1}$).³ These rates (W) were too large and showed too little dependence on d to be explained by a standard carrier tunneling model with $W \propto \exp(-\alpha d)$ (α is a constant) (Ref. 4) or dipolar coupling with $W \propto d^{-4}$.³ Surprisingly, samples with larger d showed faster anti-Stokes transfer rates than those with smaller d .³ For Stokes transfer, however, the observed rates were nearly independent of d . In this paper, we present a theoretical explanation for the principal characteristics of these intriguing data.

The anomalously large energy-transfer rates were also observed by Kim *et al.* and explained by carrier tunneling by

assuming large trans-barrier GaAs clusters in the Al_xGa_{1-x}As barrier.⁴ However, the statistical rate based on such a model is expected to decay rapidly with d . In this paper we present several important intrinsic mechanisms of energy transfer. Dipolar coupling, real and virtual photon-exchange coupling, and over-barrier ionization of the excitons through exciton-exciton Auger processes are examined.

The dominant Stokes energy transfer occurs through the decay of excitons in the higher-energy QW into free electron-hole pairs in the lower-energy QW, as proposed by TSK.³ However, we find that photon-exchange interaction yields much faster transfer rates than the dipolar rate for $d \geq 80 \text{ \AA}$ investigated by TSK. The radiative rate depends very slowly on d , decaying logarithmically at large d . For plane-wave excitons, this rate is small at 0 K, quickly reaches a maximum at a very low T , and decreases rapidly with T at higher T 's. For localized excitons, the rate depends sensitively on the localization radius ξ . It depends on T only through ξ and is independent of T if ξ is insensitive to T at low T 's. The predicted rates are in reasonable agreement with TSK's data. Photon exchange is recognized as a viable energy-transfer mechanism for optically active impurities in insulators.⁵ Dipolar coupling yields rates smaller at least by an order of magnitude for $d \geq 175 \text{ \AA}$ and with a stronger d^{-4} dependence. However, the dipolar rate can be larger than the radiative rate at a short distance (e.g., $d < 80 \text{ \AA}$). The calculated rate vanishes at $T = 0$, reaches a maximum, and then decays at a higher T . This T dependence of the dipolar Stokes energy-transfer rate for plane-wave excitons conflicts with the recent result of TSK's dipolar rate, which is finite at 0 K and decreases monotonically as a function of T . The physical significance of this discrepancy will be discussed later.

For anti-Stokes transfer through exchange-type (e.g., dipolar and photon-exchange) coupling, we show rigorously that thermal activation proportional to $\exp(-\Delta/k_B T)$ is necessary, in general, to overcome the energy mismatch $\varepsilon_{2\mathbf{K}_\parallel} - \varepsilon_{1\mathbf{K}_\parallel} = \Delta$ between the initial (QW1) and final (QW2) QW's contradicting the TSK's nonactivated rates based on the Förster-Dexter's spectral-overlap theory.^{6,7} Here \mathbf{K}_\parallel is the wave vector for the center-of-mass motion. The phonon-assisted rate is calculated for photon-exchange and dipolar transfer, yielding a negligibly small rate and an activated T dependence proportional to $\exp(-\Delta/k_B T)$. On the other hand, energy transfer through over-barrier ionization of the excitons via two-exciton Auger processes is shown to yield a significantly larger nonactivated rate which is independent of d . In this two-exciton collision process, one exciton becomes annihilated nonradiatively, imparting its energy to the other exciton and separating it into a free electron-hole pair over the barrier. These carriers relax subsequently to form excitons in the other QW. This rate is large enough (when the exciton density is not too small) to explain the recent data. The rate decreases rapidly with increasing ξ . Larger rates observed by TSK for a sample with larger $d=375 \text{ \AA}$ as compared to a $d=275 \text{ \AA}$ sample can be explained if one assumes a shorter ξ (e.g., rougher interfaces) or a larger exciton density for the 375- \AA sample.

This paper is organized as follows. In Sec. II we present a basic formalism and give the wave functions of the plane-wave and localized excitons and free electron-hole pairs. The Stokes energy-transfer rate is calculated in Sec. III using dipolar and photon-exchange (i.e., radiative) interactions. In Sec. IV we establish a useful field-theoretic formalism for exciton transfer by expressing the rate in terms of a correlation function, which is then evaluated using a standard diagram expansion technique. We show here that anti-Stokes transfer through a trans-barrier exchange mechanism such as dipole-dipole or photon-exchange coupling is always activated for large Δ (much greater than level widths). Anti-Stokes transfer rate is studied in Sec. V in terms of over-barrier ionization of the excitons through exciton-exciton Auger processes and also using dipolar and radiative phonon-assisted processes. The paper is summarized in Sec. VI with discussions.

II. BASIC FORMALISM

In this section a basic exciton formalism is presented. Partially employing the notations of Takagahara,¹ the quasi-two-dimensional (2D) ground ($1s$) exciton state with a wave vector \mathbf{K}_\parallel for the in-plane center-of-mass motion in the j th QW is represented as

$$|j, \mathbf{K}_\parallel\rangle = \frac{v_0}{L} \sum_{\mathbf{r}_e, \mathbf{r}_h} e^{i\mathbf{K}_\parallel \cdot \mathbf{R}_\parallel} F_j(\mathbf{r}_{e\parallel} - \mathbf{r}_{h\parallel}, z_e - z_j, z_h - z_j) \times a_{c\mathbf{r}_e}^\dagger a_{v\mathbf{r}_h} |0\rangle, \quad (2.1)$$

where $\Omega = L^3 = Nv_0$ is the sample volume, v_0 is the unit-cell volume, N is the total number of the unit cells, $|0\rangle$ signifies the ground state with an empty conduction band (c) and a filled valence band (v), and z_j is the z coordinate at the center of the QW. The envelop function F_j depends on the

depths and the widths of the QW. The creation and destruction operators $a_{c\mathbf{r}_e}^\dagger$ and $a_{c\mathbf{r}_e}$ ($a_{v\mathbf{r}_h}^\dagger$ and $a_{v\mathbf{r}_h}$) creates and destroys an electron in the conduction (valence) band at the position $\mathbf{r}_e(\mathbf{r}_h)$ in the Wannier representation. The quantity $\mathbf{R} = \alpha_e \mathbf{r}_e + \alpha_h \mathbf{r}_h$ is the position vector of the center of mass, where $\alpha_e = m_e/M$, $\alpha_h = m_h/M$, $M = m_e + m_h$, and $m_e(m_h)$ is the electron (hole) mass. A vector $\mathbf{q} = (\mathbf{q}_\parallel, q_z)$ is decomposed into components parallel (\mathbf{q}_\parallel) and perpendicular (q_z) to the QW plane. We define $q = |\mathbf{q}|$ and $q_\parallel = |\mathbf{q}_\parallel|$ as the absolute magnitudes of the vectors.

Converting the \mathbf{r}_σ summation into integration

$$\sum_{\mathbf{r}_\sigma} \rightarrow \frac{1}{v_0} \int d^3 r_\sigma, \quad \sigma = e, h \quad (2.2)$$

we obtain the normalization conditions $\langle j', \mathbf{K}'_\parallel | j, \mathbf{K}_\parallel \rangle = \delta_{j,j'} \delta_{\mathbf{K}'_\parallel, \mathbf{K}_\parallel}$ and

$$\int d^2 r_\parallel \int dz_e \int dz_h |F_j(\mathbf{r}_\parallel, z_e, z_h)|^2 = 1, \quad (2.3)$$

for $|j, \mathbf{K}_\parallel\rangle$ where $\mathbf{r}_\parallel = \mathbf{r}_{e\parallel} - \mathbf{r}_{h\parallel}$. The overlap of the confinement wave functions between the two QW's is neglected.

A localized exciton at site \mathbf{R}_a in the j th QW is represented by

$$|j, \mathbf{R}_a\rangle = v_0 \sum_{\mathbf{r}_e, \mathbf{r}_h} G(\mathbf{R}_\parallel - \mathbf{R}_a) \times F_j(\mathbf{r}_{e\parallel} - \mathbf{r}_{h\parallel}, z_e - z_j, z_h - z_j) a_{c\mathbf{r}_e}^\dagger a_{v\mathbf{r}_h} |0\rangle, \quad (2.4)$$

where the normalized center-of-mass wave function $G(\mathbf{R}_\parallel)$ is approximated by a Gaussian function with a localization radius ξ ,

$$G(\mathbf{R}_\parallel) = \frac{1}{\xi \sqrt{\pi}} \exp(-R_\parallel^2 / \xi^2). \quad (2.5)$$

Equations (2.1), (2.4), and the normalization conditions yield,

$$\langle j, \mathbf{K}_\parallel | j', \mathbf{R}_a \rangle = \frac{2\sqrt{\pi}\xi}{L} \exp(-i\mathbf{K}_\parallel \cdot \mathbf{R}_a - \frac{1}{2}\xi^2 K_\parallel^2) \delta_{j,j'}. \quad (2.6)$$

To obtain a numerical estimate of the transfer rate, we use, for the envelop function $F_j(\mathbf{r}_\parallel, z_e, z_h)$, a product of the 2D exciton radial wave function $F(\mathbf{r}_\parallel)$ and the quasi-2D confinement function $F_j(z_e, z_h)$,

$$F_j(\mathbf{r}_\parallel, z_e, z_h) = F(\mathbf{r}_\parallel) F_j(z_e, z_h), \quad (2.7a)$$

where

$$F(\mathbf{r}_\parallel) = \frac{2\sqrt{2}}{\sqrt{\pi} a_B} e^{-2r_\parallel / a_B}, \quad (2.7b)$$

$$F_j(z_e, z_h) = \phi_{ej}(z_e) \phi_{hj}(z_h), \quad (2.7c)$$

and $a_B = \kappa \hbar^2 / (\mu e^2)$ is the bulk exciton Bohr radius. Here μ is the reduced mass and κ is the average dielectric constant.

The functions $F(\mathbf{r}_{\parallel})$, $\phi_{ej}(z)$, and $\phi_{hj}(z)$ are normalized. The approximation in Eq. (2.7b) is employed for an order of magnitude estimate of the rates. This approximation is adequate for narrow QW's. For wide QW's, the result can be improved by employing variational expressions for $F(\mathbf{r}_{\parallel}, z_e, z_h)$.^{8,19}

A free electron-hole pair moving with wave vectors $\mathbf{k}_{e\parallel}, \mathbf{k}_{h\parallel}$ with the center-of-mass motion wave vector \mathbf{K}_{\parallel} and the relative wave vector \mathbf{k}_{\parallel} is represented as

$$|j, \mathbf{K}_{\parallel}, \mathbf{k}_{\parallel}\rangle = \frac{v_0}{L^2} \sum_{\mathbf{r}_e, \mathbf{r}_h} e^{i\mathbf{K}_{\parallel} \cdot \mathbf{R}_{\parallel}} e^{-i\mathbf{k}_{\parallel} \cdot (\mathbf{r}_e - \mathbf{r}_h)} \times F_j(z_e - z_j, z_h - z_j) a_{\mathbf{r}_e}^{\dagger} a_{\mathbf{r}_h} |0\rangle, \quad (2.8)$$

where $\mathbf{k}_{e\parallel} = \alpha_e \mathbf{K}_{\parallel} - \mathbf{k}_{\parallel}$ and $\mathbf{k}_{h\parallel} = \alpha_h \mathbf{K}_{\parallel} + \mathbf{k}_{\parallel}$. Equations (2.1) and (2.8) yield

$$\begin{aligned} \langle j, \mathbf{K}_{\parallel} | j', \mathbf{K}'_{\parallel}, \mathbf{k}'_{\parallel} \rangle &= \frac{1}{L} \delta_{\mathbf{K}_{\parallel}, \mathbf{K}'_{\parallel}} \delta_{j, j'} \int d^2 r_{\parallel} \int dz_e \int dz_h e^{-i\mathbf{k}'_{\parallel} \cdot \mathbf{r}_{\parallel}} \\ &\times F_j^*(\mathbf{r}_{\parallel}, z_e, z_h) F_j(z_e, z_h). \end{aligned} \quad (2.9)$$

In the quasi-2D approximation in Eq. (2.7a), the overlap in Eq. (2.9) reduces to

$$\begin{aligned} \langle j, \mathbf{K}_{\parallel} | j', \mathbf{K}'_{\parallel}, \mathbf{k}'_{\parallel} \rangle &= \frac{1}{L} \delta_{\mathbf{K}_{\parallel}, \mathbf{K}'_{\parallel}} \delta_{j, j'} \int d^2 r_{\parallel} e^{-i\mathbf{k}'_{\parallel} \cdot \mathbf{r}_{\parallel}} F_j^*(\mathbf{r}_{\parallel}) \\ &= \frac{8\sqrt{2}\pi a_B \delta_{j, j'}}{L(k_{\parallel}^2 a_B^2 + 4)^{3/2}} \delta_{\mathbf{K}_{\parallel}, \mathbf{K}'_{\parallel}}. \end{aligned} \quad (2.10)$$

III. STOKES ENERGY TRANSFER

In this section we study the Stokes energy-transfer rates through dipolar and photon-exchange coupling and compare them with the data of TSK. The dependence of the rate on d , T , and ξ is studied. The energy transfer occurs from narrow QW1 to wide QW2. The ground sublevel of QW2 lies below that of QW1 by Δ .

A. Dipolar energy transfer

1. Dipolar coupling between the wells

Dipolar coupling arises from the electron-electron interaction Hamiltonian H_{ee} between the two QW's. Suppressing the ground-state label $|j', 0\rangle$ from $|j, \mathbf{K}_{\parallel}; j', 0\rangle \equiv |j, \mathbf{K}_{\parallel}\rangle$ and employing Eq. (2.1), the transfer matrix is derived extending Takagahara's result¹,

$$\begin{aligned} \langle 2, \mathbf{K}'_{\parallel} | H_{ee} | 1, \mathbf{K}_{\parallel} \rangle &= \delta_{\mathbf{K}_{\parallel}, \mathbf{K}'_{\parallel}} \int dz \int dz' C(\mathbf{K}_{\parallel}, R_z) F_2^*(0, z', z') F_1(0, z, z), \end{aligned} \quad (3.1a)$$

$$C(\mathbf{K}_{\parallel}, R_z) = \int d^2 R_{\parallel} e^{i\mathbf{K}_{\parallel} \cdot \mathbf{R}_{\parallel}} C(\mathbf{R}_{\parallel}, R_z), \quad (3.1b)$$

where $R_z = z - z' - d$ with $|z|, |z'| \ll d$ and

$$C(\mathbf{R}_{\parallel}, R_z) = \frac{e^2}{\kappa R^3} [\mathbf{D}_1 \cdot \mathbf{D}_2 - 3(\hat{\mathbf{R}} \cdot \mathbf{D}_1)(\hat{\mathbf{R}} \cdot \mathbf{D}_2)], \quad (3.2)$$

in the dipole approximation. Here $\mathbf{R} = (\mathbf{R}_{\parallel}, R_z)$, $\hat{\mathbf{R}} = \mathbf{R}/R$, $\mathbf{D}_j = \int d^3 r \phi_{jv}^*(\mathbf{r}) \mathbf{r} \phi_{jc}(\mathbf{r})$ is the transition dipole, and $\phi_{ja}(\mathbf{r})$ is the Wannier function with $\mathbf{r} = 0$ at the center of the cell. A 2D version of Eq. (3.1) was also studied by TSK.³

The Hamiltonian in Eq. (3.1a) allows an exciton in QW1 to be annihilated, exciting an exciton in QW2. A free electron-hole pair state $|2, \mathbf{K}'_{\parallel}, \mathbf{k}'_{\parallel}\rangle$ can be created in QW2 instead of an exciton. The Hamiltonian for this process is obtained by replacing $F_2(\mathbf{r}_{\parallel}, z_e, z_h) \rightarrow L^{-1} \exp(-i\mathbf{k}'_{\parallel} \cdot \mathbf{r}_{\parallel}) F_2(z_e, z_h)$ in Eq. (3.1a), yielding

$$\begin{aligned} \langle 2, \mathbf{K}'_{\parallel}, \mathbf{k}'_{\parallel} | H_{ee} | 1, \mathbf{K}_{\parallel} \rangle &= L^{-1} \delta_{\mathbf{K}_{\parallel}, \mathbf{K}'_{\parallel}} \int dz \int dz' C(\mathbf{K}_{\parallel}, R_z) \\ &\times F_2^*(z', z') F_1(0, z, z). \end{aligned} \quad (3.3)$$

The quantity $C(\mathbf{K}_{\parallel}, R_z)$ is the \mathbf{K}_{\parallel} component of the interaction energy between a dipole \mathbf{D}_1 in QW1 and a sheet of dipoles \mathbf{D}_2 in QW2 at a perpendicular distance R_z and equals

$$\begin{aligned} C(\mathbf{K}_{\parallel}, R_z) &= (\pi D_1 D_2 e^2 / \kappa) K_{\parallel} e^{-K_{\parallel} |R_z|} \Phi(\phi_{K_{\parallel}}), \\ \Phi(\phi_{K_{\parallel}}) &= [\cos(2\phi_{K_{\parallel}} - \phi_D) + \cos \phi_D], \end{aligned} \quad (3.4)$$

where $\phi_{K_{\parallel}}$ (ϕ_D) is the angle between \mathbf{K}_{\parallel} and \mathbf{D}_1 (\mathbf{D}_1 and \mathbf{D}_2) in the QW plane. The expression in Eq. (3.4) vanishes in the limit $K_{\parallel} \rightarrow 0$ contradicting the result of TSK: The interaction energy of a single dipole with a sheet (or line) of uniform dipoles vanishes as well known.¹⁰ The derivation of Eq. (3.4) is given in Appendix A.¹¹

Employing the quasi-2D approximation introduced in Eq. (2.7a) and inserting Eq. (3.4) in Eqs. (3.1a) and (3.3), we obtain

$$\langle 2, \mathbf{K}'_{\parallel} | H_{ee} | 1, \mathbf{K}_{\parallel} \rangle = \frac{8D_1 D_2 e^2}{\kappa a_B^2} \Phi(\phi_{K_{\parallel}}) \delta_{\mathbf{K}_{\parallel}, \mathbf{K}'_{\parallel}} K_{\parallel} \langle e^{-K_{\parallel} |R_z|} \rangle, \quad (3.5a)$$

$$\langle e^{-K_{\parallel} |R_z|} \rangle = \int dz \int dz' F_2^*(z', z') F_1(z, z) e^{-K_{\parallel} |z - z' - d|}, \quad (3.5b)$$

and

$$\begin{aligned} \langle 2, \mathbf{K}'_{\parallel}, \mathbf{k}'_{\parallel} | H_{ee} | 1, \mathbf{K}_{\parallel} \rangle &= \frac{2\sqrt{2}\pi D_1 D_2 e^2}{a_B \kappa L} \Phi(\phi_{K_{\parallel}}) \delta_{\mathbf{K}_{\parallel}, \mathbf{K}'_{\parallel}} K_{\parallel} \langle e^{-K_{\parallel} |R_z|} \rangle, \end{aligned} \quad (3.6)$$

where $\langle \exp(-K_{\parallel} |R_z|) \rangle$ is the average over the electron and hole distribution. For an order of magnitude estimate, a rectangular distribution over the well widths b_1 and b_2 is employed, yielding ($t = K_{\parallel} d$),

TABLE I. Sample parameters for the GaAs/Al_{0.3}Ga_{0.7}As quantum wells employed in the text.

| | | | |
|----------------------|------------|-----------------------------------|-------------------|
| Electron mass m_e | $0.067m_0$ | Dielectric constant κ | 12.4 |
| Hole mass m_e | $0.14m_0$ | 3D exciton binding energy E_B^* | 4.06 meV |
| Total mass M | $0.207m_0$ | Dipole moment $D_1=D_2$ | 5.5 \AA |
| Band gap E_g | 1.52 eV | Energy mismatch Δ | 60.0 meV |
| Refractive index n | 3.68 | LO phonon energy | 36.2 meV |

$$\langle e^{-K_{\parallel}|R_z|} \rangle = e^{-t} S(t), \quad S(t) = \frac{\sinh(tb_1/2d) \sinh(tb_2/2d)}{tb_1/2d \quad tb_2/2d}. \quad (3.7)$$

The quantity $\Phi(\phi_{\mathbf{K}_{\parallel}})$ is to be squared and averaged over $\phi_{\mathbf{K}_{\parallel}}$ later, yielding

$$\frac{1}{2\pi} \int_0^{2\pi} \Phi(\phi_{\mathbf{K}_{\parallel}})^2 d\phi_{\mathbf{K}_{\parallel}} + \left(\phi_D \rightarrow \phi_D + \frac{\pi}{2} \right) = 2. \quad (3.8)$$

The transfer rate includes the contribution from the perpendicular $\mathbf{D}_2 \perp \mathbf{D}_1$ given by the second term in Eq. (3.8).³

2. Direct energy transfer from localized to plane-wave exciton states

A direct transition from $|1, \mathbf{K}_{\parallel}\rangle$ to $|2, \mathbf{K}'_{\parallel}\rangle$ is impossible because momentum ($\mathbf{K}'_{\parallel} = \mathbf{K}_{\parallel}$) and energy cannot be conserved simultaneously. Momentum conservation can be relaxed for localized initial exciton states, yielding

$$W = \frac{2\pi}{\hbar} \sum_{\mathbf{K}'_{\parallel}} |\langle 2, \mathbf{K}'_{\parallel} | H_{ee} | 1, \mathbf{R}_a \rangle|^2 \delta(E_{\mathbf{K}'_{\parallel}} - \Delta), \quad (3.9a)$$

where $E_{\mathbf{K}_{\parallel}} = \hbar^2 K_{\parallel}^2 / 2M^2$. Here we ignore the energy distribution of the localized excitons. The energy of localized excitons with ξ is of the order of $\hbar^2 / 2\xi^2 M^2 \approx 1.8 \text{ meV} \ll \Delta$ for $\xi = 100 \text{ \AA}$ and is neglected. This rate is evaluated using Eqs. (2.6) and (3.5) and (3.8) and equals

$$W = (K_{\Delta} \xi)^2 W_0 e^{-(K_{\Delta} \xi)^2} \langle e^{-K_{\Delta}|R_z|} \rangle^2, \quad (3.9b)$$

where $W_0 = 512\pi M (D_1 D_2 e^2 / \kappa a_B^2) / \hbar^3 = 2.14 \times 10^{11} \text{ sec}^{-1}$ for $a_B = 144.5 \text{ \AA}$. The parameters employed are summarized in Table I.³ In Eq. (3.9b), $(\hbar K_{\Delta})^2 / 2M = \Delta$, yielding $K_{\Delta} = 1/17.5 \text{ \AA}$ for $\Delta = 60 \text{ meV}$. Therefore, $\langle \exp(-K_{\Delta}|R_z|) \rangle^2$ is of the order of $\exp(-2dK_{\Delta}) = 2.06 \times 10^{-9}$ for $d = 175 \text{ \AA}$, yielding a negligibly small rate for all ξ for large d and Δ .

3. Energy transfer from plane-wave excitons to free electron-hole pairs

An exciton $|1, \mathbf{K}_{\parallel}\rangle$ decays into a free electron-hole pair $|2, \mathbf{K}'_{\parallel}, \mathbf{k}'_{\parallel}\rangle$ with a rate

$$W = \frac{2\pi}{\hbar} \beta \int dE_{\mathbf{K}_{\parallel}} e^{-\beta E_{\mathbf{K}_{\parallel}}} \times \left\langle \sum_{\mathbf{K}'_{\parallel}, \mathbf{k}'_{\parallel}} |\langle 2, \mathbf{K}'_{\parallel}, \mathbf{k}'_{\parallel} | H_{ee} | 1, \mathbf{K}_{\parallel} \rangle|^2 \delta(\varepsilon_{\mathbf{K}'_{\parallel}} - \Delta') \right\rangle_{\mathbf{K}_{\parallel}}, \quad (3.10)$$

where $\varepsilon_{\mathbf{k}_{\parallel}} = \hbar^2 k_{\parallel}^2 / 2\mu$, $\beta = 1/k_B T$, $\Delta' = \Delta - E_B (> 0)$, E_B is the exciton binding energy, and $\beta \int dE e^{-\beta E}$ is the Boltzmann average over the initial states. The angular brackets denote the angular average over the direction of \mathbf{K}_{\parallel} . In this process, the center-of-mass energy is conserved. The extra energy Δ' is dissipated into the relative motion of the electron and hole.

Inserting Eqs. (3.6)–(3.8) in Eq. (3.10), carrying out the \mathbf{k}'_{\parallel} summation, we find

$$W = W_{0, \text{dip}}(\xi_T) g\left(\frac{d}{\xi_T}\right), \quad (3.11a)$$

$$g(t) = \int_0^{\infty} x^3 e^{-x^2} e^{-2tx} S(tx)^2 dx,$$

$$W_{0, \text{dip}}(\xi_T) = \frac{32\pi\mu}{\hbar^3} \left(\frac{e^2 D_1 D_2}{\kappa a_B \xi_T} \right)^2, \quad (3.11b)$$

$$\xi_T = \sqrt{\frac{\hbar^2}{2Mk_B T}} = \frac{462}{\sqrt{T}} \text{ \AA} \quad (M = 0.207m_0), \quad (3.11c)$$

where T is in degrees Kelvin. Using the parameters in Table I, we estimate $W_{0, \text{dip}} = 2.87 \times 10^8 T \text{ sec}^{-1}$. The rate is plotted in Fig. 1 as a function of T for $d = 175, 375 \text{ \AA}$ and for $b_1 = 50 \text{ \AA}$, $b_2 = 100 \text{ \AA}$ as well as for $b_1 = b_2 = 0$. It is seen there

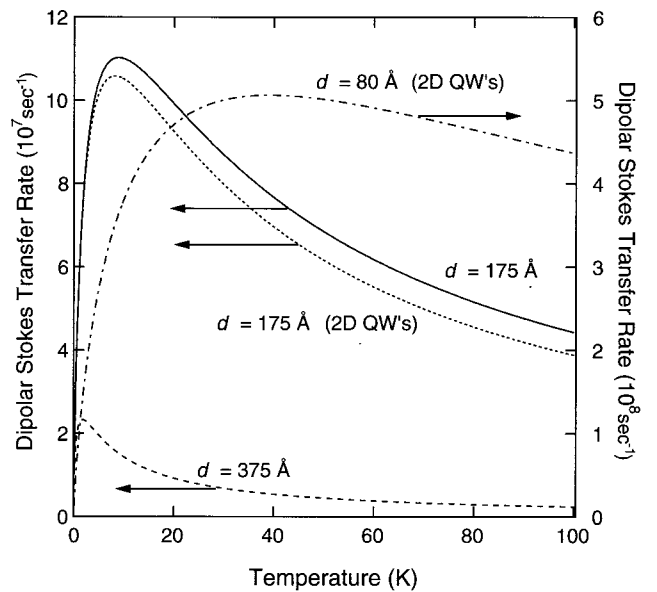


FIG. 1. Dipolar Stokes transfer rate for plane-wave excitons from a 50- \AA QW to a 100- \AA QW separated by $d = 175$ and 375 \AA with a 60-meV energy mismatch. The dotted and dash-dotted curves are for the 2D limit.

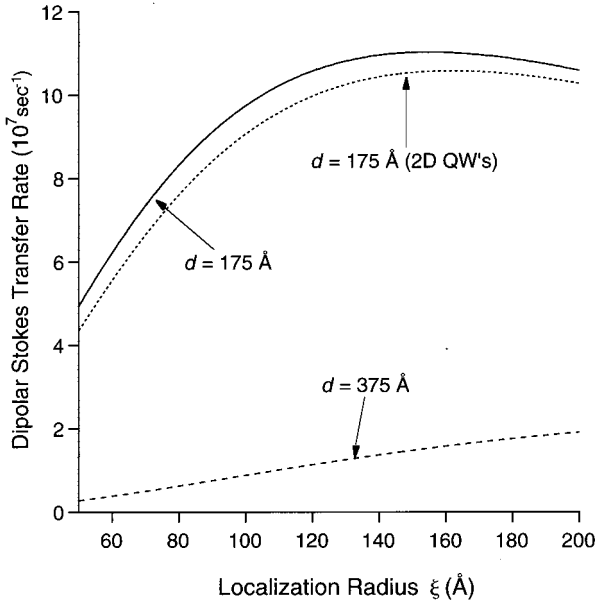


FIG. 2. Dipolar Stokes transfer rate for localized excitons from a 50-Å QW to a 100-Å QW separated by $d = 175$ and 375 Å with a 60-meV energy mismatch. The dotted curve is for the 2D limit.

that the effect of the well width is small. The rate vanishes linearly with T for $T \rightarrow 0$ because $C(\mathbf{K}_{\parallel}, R_z) \propto K_{\parallel}$ for $K_{\parallel} \rightarrow 0$ in contrast to TSK's result. The calculated rates for $d = 175$ Å (375 Å) are about one order (two orders) of magnitude smaller than TSK's data, which are insensitive to d and T . However, the rate for a much shorter distance is much larger as shown by the dash-dotted curve on the right axis for $d = 80$ Å.

4. Energy transfer from localized excitons to free electron-hole pairs

The results displayed in Fig. 1 show a rapid T dependence in contrast to TSK's data. We now show that the T dependence is absent for localized excitons. The rate for localized excitons equals

$$W = \frac{2\pi}{\hbar} \sum_{\mathbf{k}'_{\parallel}, \mathbf{k}'_{\perp}} |\langle 2, \mathbf{K}'_{\parallel}, \mathbf{k}'_{\perp} | H_{ee} | 1, \mathbf{R}_a \rangle|^2 \delta(\varepsilon_{\mathbf{k}'_{\parallel}} + E_{\mathbf{K}'_{\parallel}} - \Delta'). \quad (3.12)$$

Ignoring the distribution of ξ , W is evaluated using Eq. (2.6) and Eqs. (3.6)–(3.8) for large Δ' ,

$$W = W_{0,\text{dip}}(\xi) g\left(\frac{d}{\xi}\right), \quad (3.13)$$

which has the same form as in Eq. (3.11) except that ξ_T is replaced by ξ . The rate is plotted as a function of ξ in Fig. 2 for $d = 175, 375$ Å and for $b_1 = 50$ Å, $b_2 = 100$ Å, and $b_1 = b_2 = 0$. The rate becomes maximum at about $\xi = 140$ Å for $d = 175$ Å. The maximum occurs at a larger ξ for $d = 375$ Å (not shown in Fig. 2). These rates are of the same order of magnitude as those shown in Fig. 1 and are too small to explain the data.

B. Photon-exchange energy transfer

1. Exciton-photon coupling

The electrons see the photon field through the Hamiltonian¹²

$$H_{\text{ph}} = -\frac{e}{m_0 c} \mathbf{A} \cdot \mathbf{p},$$

$$A = i \sum_{\mathbf{k}, \lambda} \left[\frac{2\pi c^2 \hbar}{\Omega \varepsilon \omega_{\lambda \mathbf{k}}} \right]^{1/2} [b_{\lambda \mathbf{k}} e^{i\mathbf{k} \cdot \mathbf{r}} - b_{\lambda \mathbf{k}}^{\dagger} e^{-i\mathbf{k} \cdot \mathbf{r}}] \hat{\mathbf{e}}_{\lambda \mathbf{k}}, \quad (3.14)$$

where $\mathbf{p} = (m_0 / i\hbar) \int \psi^{\dagger}(\mathbf{r}) [\mathbf{r}, H_0] \psi(\mathbf{r}) d^3 r$, $\psi(\mathbf{r})$ is the field operator¹, $b_{\lambda \mathbf{k}}^{\dagger} (b_{\lambda \mathbf{k}})$ creates (destroys) a photon with mode λ, \mathbf{k} , frequency $\omega_{\lambda \mathbf{k}} = k\bar{c} = kc/n$, polarization $\hat{\mathbf{e}}_{\lambda \mathbf{k}}$, and $\varepsilon = n^2$ (n is the refractive constant). H_0 is the single-particle Hamiltonian.

The exciton-photon coupling is obtained inserting Eq. (2.1) into Eq. (3.14),

$$\begin{aligned} & \langle j, 0, N_{\lambda \mathbf{k}} + 1 | H_{\text{ph}} | j, \mathbf{K}_{\parallel}, N_{\lambda \mathbf{k}} \rangle \\ &= \frac{e E_g L}{\hbar c} \left[\frac{2\pi c^2 \hbar (N_{\lambda \mathbf{k}} + 1)}{\Omega \varepsilon \omega_{\lambda \mathbf{k}}} \right]^{1/2} \delta_{\mathbf{K}_{\parallel}, \mathbf{k}_{\parallel}} \\ & \times e^{-ik_z z_j} \hat{\mathbf{e}}_{\lambda \mathbf{k}} \cdot \mathbf{D}_j \int e^{-ik_z z} F_j(0, z, z) dz, \end{aligned} \quad (3.15)$$

where $N_{\lambda \mathbf{k}}$ is the photon occupation number and E_g is the effective gap energy.

The Hamiltonian for the creation of a free electron-hole pair through absorption of a photon is similarly obtained by inserting Eq. (2.8) into Eq. (3.14) and equals

$$\begin{aligned} & \langle j, \mathbf{K}'_{\parallel}, \mathbf{k}'_{\perp}, N_{\lambda \mathbf{k}} | H_{\text{ph}} | j, 0, N_{\lambda \mathbf{k}} + 1 \rangle \\ &= \frac{e E_g}{\hbar c} \left[\frac{2\pi c^2 \hbar (N_{\lambda \mathbf{k}} + 1)}{\Omega \varepsilon \omega_{\lambda \mathbf{k}}} \right]^{1/2} \delta_{\mathbf{K}'_{\parallel}, \mathbf{k}_{\parallel}} \\ & \times e^{ik_z z_j} \hat{\mathbf{e}}_{\lambda \mathbf{k}} \cdot \mathbf{D}_j^* \int e^{ik_z z} F_j^*(z, z) dz. \end{aligned} \quad (3.16)$$

Note that \mathbf{k}'_{\parallel} represents the in-plane wave vector for the relative motion of the electron and the hole, while \mathbf{k} is the photon wave vector. The expression in Eq. (3.16) is independent of \mathbf{k}'_{\perp} . The range dependence of the photon-exchange interaction is introduced through the phase factors $\exp(\pm ik_z z_j)$ in Eqs. (3.15) and (3.16) as will be seen later.

2. Energy transfer from localized excitons to free electron-hole pairs

A localized exciton in QW1 decays into a free electron-hole pair in QW2 through photon-exchange interaction by a two-step process at a rate

$$W = \frac{2\pi}{\hbar} \sum_{\mathbf{k}'_{\parallel}, \mathbf{K}'_{\parallel}} |T_{12,a}|^2 \delta(\varepsilon_{\mathbf{k}'_{\parallel}} + E_{\mathbf{K}'_{\parallel}} - \Delta'), \quad (3.17)$$

where

$$T_{12,a} = \sum_{\mathbf{k}} \frac{\langle 2, \mathbf{K}'_{\parallel}, \mathbf{k}'_{\parallel}, N_{\lambda\mathbf{k}} | H_{\text{ph}} | 2, 0, N_{\lambda\mathbf{k}} + 1 \rangle \langle 1, 0, N_{\lambda\mathbf{k}} + 1 | H_{\text{ph}} | 1, R_a, N_{\lambda\mathbf{k}} \rangle}{E_g - \hbar \omega_{\lambda\mathbf{k}} - i\Gamma}. \quad (3.18)$$

Here, $N_{\lambda\mathbf{k}}=0$ and Γ is the exciton damping. The t matrix in Eq. (3.18) describes a process where a photon is spontaneously emitted from an exciton in QW1 and reabsorbed in QW2, exciting a free electron-hole pair. Because $T_{12,a}$ is independent of \mathbf{k}'_{\parallel} , the \mathbf{k}'_{\parallel} summation in Eq. (3.17) can be carried out immediately, yielding

$$W = \frac{L^4 \mu}{4\pi^2 \hbar^3} \int d^2 K'_{\parallel} |T_{12,a}|^2 \theta(\Delta' - E_{\mathbf{K}'_{\parallel}}), \quad (3.19)$$

where $\theta(x)$ is the unit step function.

Inserting Eqs. (2.6), (3.15), and (3.16) in Eq. (3.18), we find

$$T_{12,a} = \frac{8\sqrt{2}\xi E_g e^2 D_1 D_2}{\hbar L^2 c n a_B} e^{-i\mathbf{K}'_{\parallel} \cdot \mathbf{R}_a} e^{-\xi^2 K'_{\parallel}{}^2/2} Q(\mathbf{K}'_{\parallel}, d), \quad (3.20)$$

$$Q(\mathbf{K}'_{\parallel}, d) = \frac{\sqrt{\pi} a_B E_g}{4\sqrt{2}} \int_{-\infty}^{\infty} dk_z e^{ik_z d} \times \frac{\int dz F_1(0, z, z) e^{-ik_z z} \int dz' F_2(z', z') e^{ik_z z'}}{(E_g - \hbar \tilde{c} \sqrt{K'_{\parallel}{}^2 + k_z^2} - i\Gamma) \sqrt{K'_{\parallel}{}^2 + k_z^2}} \times P(\mathbf{K}'_{\parallel}, k_z), \quad (3.21)$$

where

$$P(\mathbf{K}'_{\parallel}, k_z) = \sum_{\lambda} (\hat{\mathbf{e}}_{\lambda}(\mathbf{K}'_{\parallel}, k_z) \cdot \hat{\mathbf{D}}_1) (\hat{\mathbf{e}}_{\lambda}(\mathbf{K}'_{\parallel}, k_z) \cdot \hat{\mathbf{D}}_2), \quad (3.22)$$

and $\hat{\mathbf{D}}_j = \mathbf{D}_j / D_j$. The dominant contribution to the k_z integration in Eq. (3.21) arises from $\hbar \omega_{\lambda\mathbf{k}} \leq E_g$, namely from $k_z \leq \xi_g^{-1}$ where $\xi_g = \hbar \tilde{c} / E_g = 353 \text{ \AA}$ for $n=3.68$.¹³ Therefore, the phase factors in the z, z' integrations in Eq. (3.21) are roughly unity because $|z| < b_1 \ll \xi_g$, $|z'| < b_2 \ll \xi_g$, yielding unity for the z' integration. Employing a quasi-2D approximation in Eq. (2.7): $F_1(0, z, z) = 2(2/\pi)^{1/2} F_1(z, z) / a_B$, we simplify Eq. (3.21) as

$$Q(\mathbf{K}'_{\parallel}, d) = \int_0^{\infty} dk_z \cos(k_z d) \times \left(\frac{1}{(E_g / \hbar \tilde{c} - \sqrt{K'_{\parallel}{}^2 + k_z^2} - i\Gamma / \hbar \tilde{c})} + \frac{1}{\sqrt{K'_{\parallel}{}^2 + k_z^2}} \right) \times P_{\mathbf{K}'_{\parallel}, k_z}. \quad (3.23)$$

The angular integration in $\phi_{\mathbf{K}'_{\parallel}}$, in Eq. (3.19) yields, when summed over $\mathbf{D}_1 \parallel \mathbf{D}_2$ and $\mathbf{D}_1 \perp \mathbf{D}_2$,

$$\frac{1}{2\pi} \int_0^{2\pi} d\phi_{\mathbf{K}'_{\parallel}} \sum_{\parallel, \perp} P(\mathbf{K}'_{\parallel}, k'_z) P(\mathbf{K}'_{\parallel}, k_z) = \frac{1}{2} \left[1 + \frac{k_z^2 k_z'^2}{K'^2 K'^2} \right], \quad (3.24)$$

where $K^2 = K'_{\parallel}{}^2 + k_z^2$ and $K'^2 = K'_{\parallel}{}^2 + k_z'^2$.

Inserting Eqs. (3.20)–(3.24) in Eq. (3.19), we find

$$W = \frac{W_{0,\text{rad}}}{2\pi^2} \int_0^{\infty} dx \theta(\xi^2 / \xi_{\Delta'}^2 - x) e^{-x} \times [|I_0(xd^2 / \xi^2)|^2 + |I_1(xd^2 / \xi^2)|^2], \quad (3.25)$$

$$I_n(x) = \int_0^{\infty} dz \frac{z^{2n} \cos z}{[x + z^2]^n} \left\{ \frac{1}{\sqrt{x + z^2}} + \frac{1}{\frac{d}{\xi_g} - \sqrt{x + z^2} - i\gamma} \right\}, \quad (3.26)$$

where $W_{0,\text{rad}} = 32\pi\mu(E_g e^2 D_1 D_2)^2 / (\hbar^5 c^2 \epsilon a_B^2)$, $\xi_{\Delta'}^2 = \hbar^2 / (2M\Delta')$ and $\gamma = \Gamma d / \hbar \tilde{c} = (\Gamma / E_g)(d / \xi_g) \ll 1$. For GaAs, $\xi_{\Delta'} = 18.1 \text{ \AA}$ for $\Delta = 60 \text{ meV}$. Using Table I, we estimate $W_{0,\text{rad}} = 3.64 \times 10^8 \text{ sec}^{-1}$. The rate in Eq. (3.25) is independent of b_1, b_2 for $b_1, b_2 \ll \xi_g$.

The rate in Eq. (3.25) is the sum of the nonresonant and resonant contributions, i.e., $W = W_{\text{nrs}} + W_{\text{res}}$. Here W_{nrs} is from the principal part of Eq. (3.26) while W_{res} is from the imaginary part given by

$$W_{\text{res}} = \frac{W_{0,\text{rad}}}{2} \int_0^{\infty} dx \theta(\xi^2 / \xi_{\Delta'}^2 - x) \theta(\xi^2 / \xi_g^2 - x) \times e^{-x} \cos^2 \left(\frac{d}{\xi} \sqrt{(\xi / \xi_g)^2 - x} \right) \times \left\{ \frac{(\xi / \xi_g)^2}{(\xi / \xi_g)^2 - x + \gamma} + (\xi_g / \xi)^2 [(\xi / \xi_g)^2 - x] \right\}. \quad (3.27)$$

Here small γ is inserted to avoid a weak logarithmic divergence. W_{res} reduces to $W_{\text{res}} = W_{0,\text{rad}} \cos^2(d / \xi_g)$ for $\xi \gg \xi_g$, ξ_{Δ}' and to $W_{\text{res}} = W_{0,\text{rad}} \{ \ln[(\xi^2 / \xi_g^2 + \gamma) / \gamma] + \frac{1}{2} \xi^2 / (2\xi_g^2) \}$ for $\xi_g \gg \xi, \xi_{\Delta}', d$. The real part of the integral in Eq. (3.26) is calculated excluding the region $|x - x_s| < \gamma$ around the singularity point x_s . We use $\Gamma = 0.01 \text{ meV}$ corresponding to the lifetime of about 100 psec (Ref. 3) for the numerical analysis presented below. This value corresponds to $\gamma = 3.26 \times 10^{-6}$ for $d = 175 \text{ \AA}$. The rate increases (decreases) by about 25% when γ is reduced (increased) by an order of magnitude.

Figure 3(a) displays W_{res} , W_{nrs} , and W as a function of ξ for $d = 175 \text{ \AA}$. W_{res} and W_{nrs} are equally important and have maxima near $\xi \sim \xi_g$, where $\hbar \omega_k$ (with $k \sim \xi^{-1}$) $\sim E_g$. W is insensitive to d as shown in Fig. 3(b) as a function of ξ (lower axis) for $d = 175, 275, 375 \text{ \AA}$ and also in Fig. 4. W is independent of T for T -independent ξ and is in the range of TSK's Stokes transfer rate data³ shown as a function of T (upper axis) in Fig. 3(b). The calculated W is also plotted as a function of d in Fig. 4 for $\xi = 150, 400$, and 1500 \AA . W has a very slow dependence on d in agreement with TSK's data. W_{res} vanishes near $d = \pi \xi_g / 2 = 554 \text{ \AA}$ for large ξ

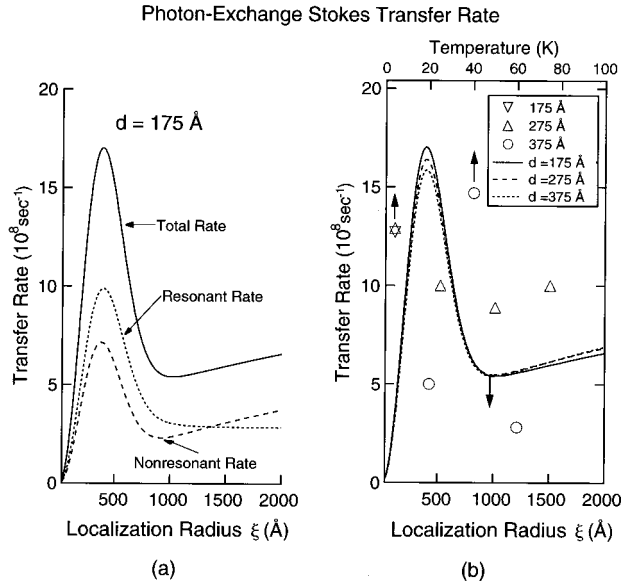


FIG. 3. Photon-exchange Stokes transfer rate for localized excitons from a narrow to a wide QW separated by (a) $d = 175$ and (b) $d = 175$ – 375 \AA with a 60-meV energy mismatch. Contributions from the resonant and nonresonant processes are shown in (a). Temperature-dependent data (symbols) of TSK (Ref. 3) are shown in (b) in the upper axis.

$= 1500 \gg \xi_g = 353 \text{ \AA}$ (not shown in Fig. 4) as predicted by $W_{\text{res}} = W_{0,\text{rad}} \cos^2(d/\xi_g)$ and creates a shallow maximum for W near $d = 350 \text{ \AA}$ as seen in Fig. 4. It is possible from Figs. 3 and 4 that samples with a larger d can have faster rates depending on ξ .

3. Energy transfer from plane-wave excitons to free electron-hole pairs

The transfer rate from a plane-wave exciton state in QW1 to a free electron-hole pair in QW2 can be obtained from the formalism in Sec. III B 2. The rate is given by

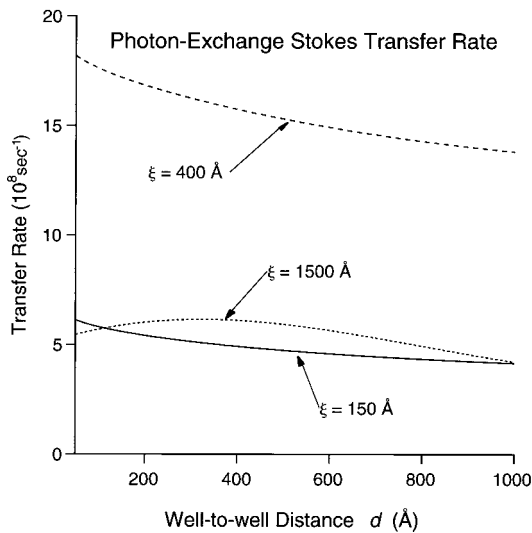


FIG. 4. Photon-exchange Stokes transfer rate as a function of the well-to-well separation d for localized excitons from a narrow to a wide QW with a 60-meV energy mismatch for the exciton localization radius $\xi = 150, 400,$ and 1500 \AA .

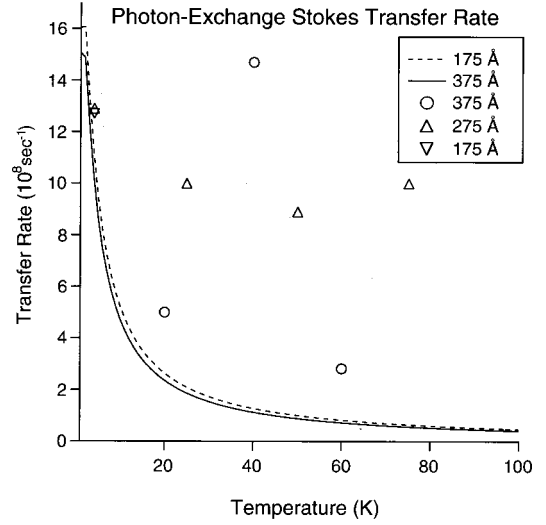


FIG. 5. Photon-exchange Stokes transfer rate as a function of the temperature for plane-wave excitons from a narrow to a wide QW separated by $d = 175$ and 375 \AA with a 60-meV energy mismatch. The symbols indicate the data from TSK (Ref. 3).

$$W = \frac{2\pi}{\hbar} \beta \int dE_{\mathbf{k}_{\parallel}} e^{-\beta E_{\mathbf{k}_{\parallel}}} \times \left\langle \sum_{\mathbf{k}'_{\parallel}, \mathbf{k}_{\parallel}} |T_{12}(\mathbf{K}'_{\parallel}, \mathbf{K}_{\parallel})|^2 \delta(\varepsilon_{\mathbf{k}'_{\parallel}} - \Delta') \right\rangle_{\mathbf{K}_{\parallel}}, \quad (3.28)$$

where the $T_{12}(\mathbf{K}'_{\parallel}, \mathbf{K}_{\parallel})$ is obtained by replacing $|1, \mathbf{R}_d, N_{\lambda \mathbf{k}}\rangle$ with $|1, \mathbf{K}_{\parallel}, N_{\lambda \mathbf{k}}\rangle$ in $T_{12,a}$ in Eq. (3.18). The Boltzmann average is taken over the initial energy $E_{\mathbf{k}_{\parallel}}$ in Eq. (3.28). The unit step function $\theta(\xi^2/\xi_{\Delta}^2 - x)$ in Eqs. (3.25)–(3.27) is not necessary and should be replaced by unity. Otherwise, the rate in Eq. (3.28) reduces to Eqs. (3.25)–(3.27) except that ξ is replaced with ξ_T defined in Eq. (3.11c), namely,

$$W = \frac{W_{0,\text{rad}}}{2\pi^2} \int_0^{\infty} dx e^{-x} [|I_0(xd^2/\xi_T^2)|^2 + |I_1(xd^2/\xi_T^2)|^2]. \quad (3.29)$$

For the numerical results shown in Figs. 3 and 4, the cutoff factor $\theta(\xi^2/\xi_{\Delta}^2 - x)$ in Eq. (3.25) has a negligible effect because ξ^2/ξ_{Δ}^2 is very large. Therefore, the rates displayed in Figs. 3 and 4 can be directly translated into T -dependent rates by equating $\xi = \xi_T = 462/T^{1/2} \text{ \AA}$, where T is in degrees Kelvin. The energy transfer rate is shown as a function of T in Fig. 5 for $d = 175$ and 375 \AA . The rapid decay with rising T is consistent with the steep decay with decreasing ξ below the maximum in Fig. 3 in view of $\xi = \xi_T = 462/T^{1/2} \text{ \AA}$. We can also deduce from Fig. 3 that the rate has a maximum near $\xi_T = 390 \text{ \AA}$, namely near 1.4 K in Fig. 5. The rapid T -dependent decay at high T is due to the fact that the photon energy in the denominators of Eq. (3.23) becomes large. Figure 6 displays the d dependence of the rate at $T = 4, 10,$ and 50 K .

The radiative rate in Figs. 4 and 6 decays very slowly for extremely large d . We show in Appendix B that the asymptotic behavior depends on the sample shape. The rate saturates to an asymptotic value independent of d in a long

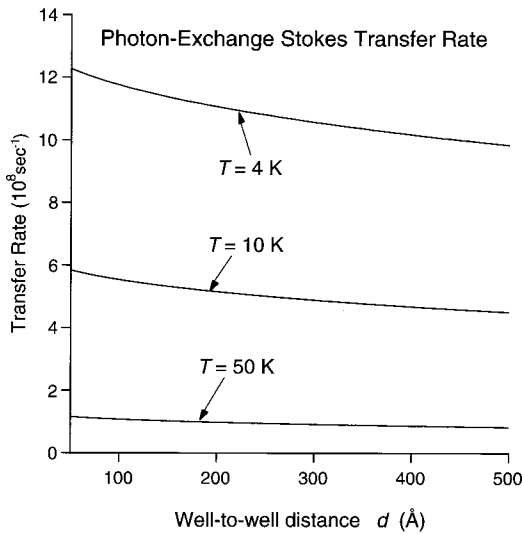


FIG. 6. Photon-exchange Stokes transfer rate as a function of the well-to-well separation d for plane-wave excitons from a narrow to a wide QW with a 60-meV energy mismatch for $T=4, 10,$ and 50 K.

sample where d is much larger than the radii of the QW's. In the opposite limit, the rate slows down logarithmically. However, the rate is limited by the photon mean free path if there are other optical-absorbing centers present in the system.

IV. FIELD-THEORETIC FORMALISM FOR EXCITON TRANSFER

A. Formalism

In this section we express the transfer rate in terms of a correlation function, which allows a rigorous and systematic calculation of the rate by using a standard diagrammatic technique. The total Hamiltonian is the sum of H_t and H ,

$$H = \sum_{jk} (\varepsilon_{jk} - \mu_j) \hat{n}_{jk} + H', \quad (4.1a)$$

$$H_t = \hat{t} + \hat{t}^\dagger. \quad (4.1b)$$

The first term of H is the energy of the exciton which is either at $j=1$ or at $j=2$ with the occupation number $\hat{n}_{jk} = 0$ or 1 . The chemical potential μ_j at site j is introduced to project out the initial unphysical occupation of site 2 later. The second term H' describes the rest of the system (e.g., phonons) and its interactions with the exciton. The operator \hat{t}^\dagger transfers an exciton from QW1 to QW2 and \hat{t} from QW2 to QW1.

The transition rate is given to the lowest order in \hat{t} by

$$W = \frac{2\pi}{\hbar Z} \sum_{nm} [e^{-\beta E_n} \langle m | \hat{t}^\dagger | n \rangle]^2 - e^{-\beta E_m} \langle n | \hat{t} | m \rangle]^2 \delta(E_n - E_m + \Omega), \quad (4.2)$$

where $H|n\rangle = E_n|n\rangle$, $\Omega = \mu_1 - \mu_2$, and Z is the distribution function for H . The first term in Eq. (4.2) describes the trans-

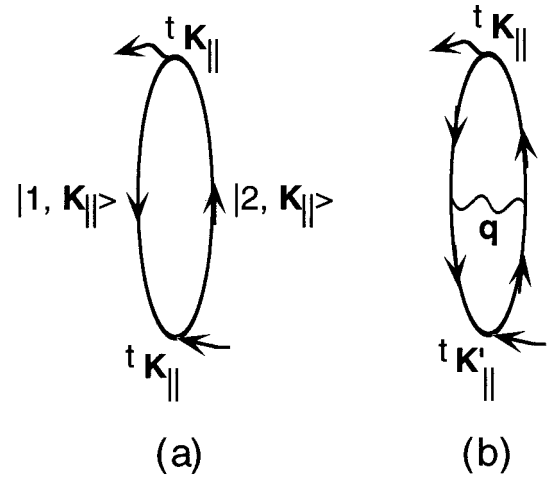


FIG. 7. Basic diagrams for the correlation function defined in Eq. (4.3) for the exciton transfer rate. The solid lines are dressed exciton propagators and the wavy line a phonon propagator. The arrows indicate the direction of momentum and energy flow. The bubble diagram (a) yields the result in Eq. (4.5) and the one-rung diagram (b) the interference term in Eq. (4.6).

fer rate from QW1 to QW2 and the second term the back transfer. To ensure that QW1 is occupied and QW2 is empty initially, we let $\Omega \rightarrow \infty$. The expression in Eq. (4.2) can be rewritten as

$$W = \frac{2}{\hbar} \text{Im} \mathcal{F}(\omega_r \rightarrow \Omega + i0),$$

$$\mathcal{F}(\omega_r) = \int_0^\beta du e^{\omega_r u} \langle e^{uH} \hat{t} e^{-uH} \hat{t}^\dagger \rangle, \quad (4.3)$$

where $\omega_r = 2\pi i r / \beta$ is analytically continued to slightly above the real axis. Here r is an integer. The angular brackets in Eq. (4.3) signify the thermodynamic average. The current correlation function in Eq. (4.3) can be evaluated systematically applying a standard temperature-ordered diagram expansion technique.^{14,15}

B. Application to anti-Stokes transfer of plane-wave excitons

The above result is useful for studying the effect of damping and scattering for anti-Stokes transfer. Since there is only one exciton in the system, we can employ a Fermion representation and write $\hat{n}_{jk} = c_{jk}^\dagger c_{jk}$ where $k = \mathbf{K}_{\parallel}$, c_{jk}^\dagger , c_{jk} are creation and destruction operators and $\hat{t}^\dagger = \sum_k t_{\mathbf{K}_{\parallel}} c_{2k}^\dagger c_{1k}$. Here $t_{\mathbf{K}_{\parallel}} = \langle 2, \mathbf{K}_{\parallel} | H_t | 1, \mathbf{K}_{\parallel} \rangle$ represents dipolar and photon-exchange coupling. We assume that the exciton interacts with phonons and other static scattering centers (e.g., surface roughness, impurities).

The rate in Eq. (4.3) is given by a bubble diagram and a one-rung diagram shown in Fig. 7, where the solid lines are dressed exciton propagators and the wavy line is a phonon propagator or a single-impurity line. The bubble diagram yields¹⁴⁻¹⁶

$$W = \frac{2\pi}{\hbar} \int_{-\infty}^{\infty} dz [f_1(z) - f_2(z)] \sum_{\mathbf{K}_{\parallel}} |t_{\mathbf{K}_{\parallel}}|^2 \rho_{1\mathbf{K}_{\parallel}}(z) \rho_{2\mathbf{K}_{\parallel}}(z), \quad (4.4a)$$

$$\rho_{j\mathbf{K}_{\parallel}}(z) = \frac{1}{\pi} \frac{\Gamma_{j\mathbf{K}_{\parallel}}(z)}{(z - E_{j\mathbf{K}_{\parallel}})^2 + \Gamma_{j\mathbf{K}_{\parallel}}(z)^2}, \quad (4.4b)$$

where $f_j(z) = \exp[-\beta(z - \mu_j)]$ is the occupation function (i.e., the Fermi function in the nondegenerate limit) and $\Gamma_{j\mathbf{K}_{\parallel}}(z)$ is the imaginary part of the self-energy. The quantity $\Gamma_{j\mathbf{K}_{\parallel}}(z)$ represents damping due to exciton interactions. The exciton shift (i.e., the real part of the self-energy) is absorbed into $E_{j\mathbf{K}_{\parallel}}$ in the spectral function in Eq. (4.4b). The second term proportional to $f_2(z)$ in Eq. (4.4a) is zero in the limit $\Omega \rightarrow \infty$ and is dropped.

In the limit $\Delta \gg \Gamma$, dominant contributions arise from the two nonoverlapping resonances at $z = E_{1\mathbf{K}_{\parallel}}$ and $z = E_{2\mathbf{K}_{\parallel}}$ in Eq. (4.4a), yielding

$$W = \frac{2}{\hbar Z_1 \Delta^2} \sum_{\mathbf{K}_{\parallel}} |t_{\mathbf{K}_{\parallel}}|^2 [e^{-\beta E_{1\mathbf{K}_{\parallel}}} \Gamma_{2\mathbf{K}_{\parallel}}(E_{1\mathbf{K}_{\parallel}}) + e^{-\beta E_{2\mathbf{K}_{\parallel}}} \Gamma_{1\mathbf{K}_{\parallel}}(E_{2\mathbf{K}_{\parallel}})], \quad (4.5)$$

where $\exp(-\beta\mu_1) = \sum_{\mathbf{K}_{\parallel}} \exp(-\beta E_{1\mathbf{K}_{\parallel}}) \equiv Z_1$ for a single-particle occupancy in QW1. The physical origin of the expression in Eq. (4.5) will be discussed later in this section.

The nonactivated result of TSK is obtained from Eq. (4.4a) by (1) replacing $f_1(z) = f_1(E_{1\mathbf{K}_{\parallel}})$ and (2) approximating the rest of the z integration by $\rho_{1\mathbf{K}_{\parallel}}(z = E_{2\mathbf{K}_{\parallel}})$. However, this step is incorrect because the occupation function should also reflect the same resonance $f_1(z) = f_1(E_{2\mathbf{K}_{\parallel}}) \propto \exp(-\beta E_{2\mathbf{K}_{\parallel}}) \propto e^{-\beta\Delta}$ rather than $f_1(z) = f_1(E_{1\mathbf{K}_{\parallel}})$.

While the second term in Eq. (4.5) is proportional to $e^{-\beta\Delta}$, the same behavior is not apparent for the first term. However, the first term in Eq. (4.5) is proportional to $e^{-\beta\Delta}$ because (1) $\Gamma_{2\mathbf{K}_{\parallel}}(E_{1\mathbf{K}_{\parallel}}) = 0$ unless K_{\parallel} is large enough to satisfy $E_{1\mathbf{K}_{\parallel}} \geq \Delta$ for elastic scattering and (2) $\Gamma_{2\mathbf{K}_{\parallel}}(E_{1\mathbf{K}_{\parallel}}) \propto e^{-\beta\Delta}$ for damping through one-phonon absorption.¹⁵ The contribution to Γ from the natural lifetime can be neglected.

The physical origin of the expression given in Eq. (4.5) can be understood by rederiving the full phonon-assisted rate in terms of an alternative standard perturbation method. The resulting rate will be employed in Sec. V. For this purpose, we consider two possible perturbation channels which connect the initial state $|1, \mathbf{K}_{\parallel}, n_{s\mathbf{q}}\rangle$ to the final state $|2, \mathbf{K}_{\parallel}, n_{s\mathbf{q}} + \frac{1}{2} \pm \frac{1}{2}\rangle$ through intermediate states via emission (+) and absorption (-) of a phonon. Here $n_{s\mathbf{q}}$ is the occupation for the phonon modes s, \mathbf{q} , and energy $\hbar\omega_{s\mathbf{q}}$. The thermally averaged rate equals

$$W = \frac{2\pi}{\hbar Z_1} \sum_{\mathbf{K}_{\parallel}} e^{-\beta E_{1\mathbf{K}_{\parallel}}} \sum_{\mathbf{K}'_{\parallel}, s\mathbf{q}\pm} |t_{12,\pm}|^2 \delta(E_{2\mathbf{K}'_{\parallel}} \pm \hbar\omega_{s\mathbf{q}} - E_{1\mathbf{K}_{\parallel}}), \quad (4.6)$$

where the t matrix is given by¹⁷

$$t_{12,\pm} = \left(\frac{t_{\mathbf{K}_{\parallel}} e^{iq_z z_2} V_{2,s\mathbf{q}} + t_{\mathbf{K}'_{\parallel}} e^{iq_z z_1} V_{1,s\mathbf{q}}}{-\Delta} + \frac{t_{\mathbf{K}'_{\parallel}} e^{iq_z z_1} V_{1,s\mathbf{q}}}{\Delta} \right) \times \left(n_{s\mathbf{q}} + \frac{1}{2} \pm \frac{1}{2} \right)^{1/2} \delta_{\mathbf{K}_{\parallel}, \mathbf{K}'_{\parallel} \pm \mathbf{q}_{\parallel}}. \quad (4.7)$$

A full expression for the exciton-phonon interaction $V_{j,s\mathbf{q}}$ will be given in Sec. V.

The first term of Eq. (4.7) describes a process where the exciton crosses the barrier through dipolar and photon-exchange interactions (i.e., via $t_{\mathbf{K}_{\parallel}}$) to an intermediate virtual state $|2, \mathbf{K}_{\parallel}, n_{s\mathbf{q}}\rangle$ and is then scattered to the final state by $V_{2,s\mathbf{q}}$ emitting and absorbing a phonon. For the second term, the exciton is scattered to an intermediate virtual state $|1, \mathbf{K}'_{\parallel}, n_{s\mathbf{q}} + \frac{1}{2} \pm \frac{1}{2}\rangle$ inside QW1 by $V_{1,s\mathbf{q}}$ emitting and absorbing a phonon and then crosses the barrier into the final state via $t_{\mathbf{K}'_{\parallel}}$. The first term of Eq. (4.5) is obtained immediately by inserting the first term of Eq. (4.7) in Eq. (4.6). The second term of Eq. (4.5) follows from the second term of Eq. (4.7). The cross terms in Eqs. (4.6) and (4.7) yield the contribution shown by the one-rung diagram in Fig. 7 and are proportional to $e^{-\beta\Delta}$ as will be shown in Sec. V. More detailed study of the total one-phonon-assisted rate will be carried out in the next section. An analogous analysis can be applied to static scattering.

V. ANTI-STOKES ENERGY TRANSFER

In this section we study exciton transfer from wide QW1 to narrow QW2. The ground sublevel of QW2 lies Δ above that of QW1. We have shown in Sec. IV that dipolar or photon-exchange anti-Stokes energy transfer is proportional to $e^{-\beta\Delta}$. As a result, the phonon-assisted rate is negligible at low T . We find that the dominant anti-Stokes energy transfer occurs through the following Auger-like exciton-exciton collision processes at a sufficiently high exciton density, yielding sufficiently large rates to explain recent data.

A. Over-barrier ionization of plane-wave excitons

An exciton in $|\mathbf{K}_{1\parallel}\rangle$ in QW1 is annihilated *nonradiatively*, ionizing another exciton $|\mathbf{K}_{2\parallel}\rangle$ in the same well over the barrier into a free electron-hole state $|\mathbf{K}'_{\parallel}, \mathbf{k}'_{\parallel}, k'_{ze}, k'_{zh}\rangle$. Once excited over the barrier, the carriers fall into QW2 “immediately” in the time much less than the transfer time $\sim 10^{-6}$ sec. Phonon-assisted carrier capture is faster in the narrower QW. The subscript j refers to the two excitons. The final unconfined free electron-hole state is described by

$$|\mathbf{K}'_{\parallel}, \mathbf{k}'_{\parallel}, k'_{ze}, k'_{zh}\rangle = \frac{v_0}{L^2} \sum_{\mathbf{r}_e, \mathbf{r}_h} e^{i\mathbf{K}'_{\parallel} \cdot \mathbf{R}_{\parallel}} e^{-i\mathbf{k}'_{\parallel} \cdot (\mathbf{r}_{e\parallel} - \mathbf{r}_{h\parallel})} \times F(k'_{ze}, z_e; k'_{zh}, z_h) a_{c\mathbf{r}_e}^{\dagger} a_{v\mathbf{r}_h} |0\rangle, \quad (5.1a)$$

where

$$F(k'_{ze}, z_e; k'_{zh}, z_h) = \phi_{e,k'_{ze}}(z_e) \phi_{h,k'_{zh}}(z_h) \quad (5.1b)$$

is the product of the normalized electron and hole wave functions that propagate above the barrier in the z direction.

Following a similar procedure employed in Eqs. (3.1)–(3.3), we find

$$\begin{aligned}
& \langle \mathbf{K}'_{\parallel}, \mathbf{k}'_{\parallel}, k'_{ze}, k'_{zh} | H_{ee} | \mathbf{K}_{1\parallel}, \mathbf{K}_{2\parallel} \rangle \\
&= \frac{1}{L^2} \delta_{\mathbf{K}_{1\parallel} + \mathbf{K}_{2\parallel}, \mathbf{K}'_{\parallel}} \int dZ \int dZ' C_{D_1}(\mathbf{K}_{1\parallel}, R_z) \\
&\quad \times F(0, Z, Z) \int d^2 r_{\parallel} \int dz' F(\mathbf{r}_{\parallel}, Z', z') \\
&\quad \times [F^*(k'_{ze}, Z'; k'_{zh}, z') e^{i(\mathbf{k}'_{\parallel} + \alpha_h \mathbf{K}_{1\parallel}) \cdot \mathbf{r}_{\parallel}} \\
&\quad - F^*(k'_{ze}, z'; k'_{zh}, Z') e^{i(\mathbf{k}'_{\parallel} - \alpha_e \mathbf{K}_{1\parallel}) \cdot \mathbf{r}_{\parallel}}] + (1 \rightarrow 2),
\end{aligned} \tag{5.2a}$$

where $R_z = Z' - Z$, $C_{D_1}(\mathbf{R}) = -e^2 \mathbf{R} \cdot \mathbf{D}_1 / \kappa R^3$ is the monopole-dipole interaction and

$$\begin{aligned}
C_{D_1}(\mathbf{K}_{\parallel}, R_z) &= \int d^2 R_{\parallel} e^{i\mathbf{K}_{\parallel} \cdot \mathbf{R}_{\parallel}} C_{D_1}(\mathbf{R}) \\
&= -\frac{2\pi i e^2}{\kappa} \hat{\mathbf{K}}_{\parallel} \cdot \mathbf{D}_1 e^{-K_{\parallel} |R_z|}.
\end{aligned} \tag{5.2b}$$

Here $\mathbf{R} = (\mathbf{R}_{\parallel}, R_z)$ and \mathbf{D}_j is that of the initial confined state $|\mathbf{K}_{j\parallel}\rangle$.

The Z, Z' integrations for the two initial exciton states in Eq. (5.2a) are sharply localized in QW1. We approximate $C_{D_1}(\mathbf{K}_{1\parallel}, R_z)$ by its average over the probability distribution of Z and Z'

$$C_{D_1}(\mathbf{K}_{\parallel}) = -\frac{2\pi i e^2}{\kappa} \hat{\mathbf{K}}_{\parallel} \cdot \mathbf{D}_1 B(K_{\parallel}), \quad B(K_{\parallel}) = \langle e^{-K_{\parallel} |Z' - Z|} \rangle, \tag{5.3}$$

where $B(K_{\parallel}) = 2(x - 1 + e^{-x})/x^2$ with $x = bK_{\parallel}$ for a rectangular distribution of the electron and hole densities and b is the width of QW1. At this point, we employ the quasi-2D approximations in Eq. (2.7) for the exciton wave function in Eq. (5.2a).

Carrying out the \mathbf{r}_{\parallel} integration for the matrix element in Eq. (5.2a), we find

$$\begin{aligned}
& \langle \mathbf{K}'_{\parallel}, \mathbf{k}'_{\parallel}, k'_{ze}, k'_{zh} | H_{ee} | \mathbf{K}_{1\parallel}, \mathbf{K}_{2\parallel} \rangle \\
&= \frac{32}{L^2} \delta_{\mathbf{K}_{1\parallel} + \mathbf{K}_{2\parallel}, \mathbf{K}'_{\parallel}} C_{D_1}(\mathbf{K}_{1\parallel}) \int dZ' \int dz' \\
&\quad \times F^*(k'_{ze}, Z'; k'_{zh}, z') F_g(Z', z') \\
&\quad \times \left[\frac{1}{[(\mathbf{k}'_{\parallel} + \alpha_h \mathbf{K}_{1\parallel})^2 a_B^2 + 4]^{3/2}} \right. \\
&\quad \left. - \frac{1}{[(\mathbf{k}'_{\parallel} - \alpha_e \mathbf{K}_{1\parallel})^2 a_B^2 + 4]^{3/2}} \right] + (1 \rightarrow 2),
\end{aligned} \tag{5.4}$$

where the subscript ‘‘g’’ is introduced to distinguish the ground-state confinement function $F_g(Z', z')$ from the over-barrier wave function, which is assumed to be symmetric in the electron and the hole coordinates.

The thermally averaged total exciton-exciton ionization rate is given by

$$\begin{aligned}
W &= \frac{2\pi}{\hbar Z_1} \sum_{\mathbf{K}_{1\parallel}, \mathbf{K}_{2\parallel}} e^{-\beta E_{\mathbf{K}_{1\parallel}}} f_{\mathbf{K}_{2\parallel}} \\
&\quad \times \sum_{\mathbf{K}'_{\parallel}, \mathbf{k}'_{\parallel}, k'_{ze}, k'_{zh}} |\langle \mathbf{K}'_{\parallel}, \mathbf{k}'_{\parallel}, k'_{ze}, k'_{zh} | H_{ee} | \mathbf{K}_{1\parallel}, \mathbf{K}_{2\parallel} \rangle|^2 \\
&\quad \times \delta(E_{\mathbf{K}_{1\parallel}} + E_{\mathbf{K}_{2\parallel}} - 2E_B + E_g \\
&\quad - [E_{\mathbf{K}'_{\parallel}} + \varepsilon_{\mathbf{k}'_{\parallel}} + \varepsilon_e(k'_{ze}) + \varepsilon_h(k'_{zh})]),
\end{aligned} \tag{5.5}$$

where $f_{\mathbf{K}_{2\parallel}} = 2\pi \hbar^2 N_{\text{ex}} \beta \exp(-\beta E_{\mathbf{K}_{2\parallel}}) / M$ is the exciton occupancy, N_{ex} is the 2D exciton density, $\varepsilon_e(k'_{ze})$, $\varepsilon_h(k'_{zh})$ are the electron, hole energies in the z direction. Because $F_g(Z', z')$ is confined inside the QW in Eq. (5.4), the Z', z' integrations yield negligible contributions for large $|k'_{ze}|$, $|k'_{zh}| > \pi/b$, which is the momentum uncertainty in the z direction. Therefore, we approximate $\varepsilon_e(k'_{ze}) + \varepsilon_h(k'_{zh}) = V_0$ in the energy δ function in Eq. (5.5) for small $|k'_{ze}|$, $|k'_{zh}| < \pi/b$, where V_0 is the sum of the well depths in the conduction and valence bands. Also, the exciton energies are of the order of the thermal energy and are neglected. The energy δ function then yields $\varepsilon_{\mathbf{k}'_{\parallel}} = E_g - V_0 - 2E_B \equiv E_g^*$. The integrations on k'_{ze} and k'_{zh} are carried out using the closure property.

The wave number k'_{\parallel} for the electron-hole relative motion in the denominators of Eq. (5.4) is much larger than $K_{1\parallel}$ because $\varepsilon_{\mathbf{k}'_{\parallel}} \gg E_{\mathbf{k}'_{\parallel}}$. This allows us to expand the two terms in the large square brackets of Eq. (5.4) to the first order in $\mathbf{K}_{1\parallel}$. We then obtain after a lengthy algebra

$$\begin{aligned}
W &= W_{0,\text{ion}}(\xi_T) \left[\int_0^{\infty} x e^{-x} B(\sqrt{x}/\xi_T)^2 dx \right. \\
&\quad \left. + \frac{1}{4} \left\{ \int_0^{\infty} \sqrt{x} e^{-x} B(\sqrt{x}/\xi_T) dx \right\}^2 \right],
\end{aligned} \tag{5.6}$$

where $W_{0,\text{ion}}(\xi_T) = (96\pi)^2 N_{\text{ex}} (e^2 D_1 / \kappa)^2 E_B^{*3} / \hbar \xi_T^2 E_g^{*4}$, and E_B^* is the bulk exciton binding energy. For the parameters in Table I, $N_{\text{ex}} = 5 \times 10^{10} \text{ cm}^{-2}$ and $E_g^* = 1.09 \text{ eV}$ corresponding to GaAs/Al_{0.3}Ga_{0.7}As, we estimate $W_{0,\text{ion}}(\xi_T) = 1.25T \times 10^4 \text{ sec}^{-1}$ where T is in Kelvin. The T dependence of the exciton ionization rate is plotted in Fig. 8 for $b = 100$ and 50 \AA . The theoretical rates are in the range of TSK's observed data. Note that the data for $d = 375 \text{ \AA}$ show faster rates than those for $d = 175 - 275 \text{ \AA}$.

B. Over-barrier ionization of localized excitons

In this case we replace the initial exciton states $|\mathbf{K}_{1\parallel}\rangle$ and $|\mathbf{K}_{2\parallel}\rangle$ in Eq. (5.5) by localized states $|\mathbf{R}_1\rangle$ and $|\mathbf{R}_2\rangle$. Final free electron-hole states $|\mathbf{K}'_{\parallel}, \mathbf{k}'_{\parallel}, k'_{ze}, k'_{zh}\rangle$ are the same. The rate in Eq. (5.5) is replaced with

$$\begin{aligned}
W &= \frac{2\pi}{\hbar} \sum_{\mathbf{R}_2} \sum_{\mathbf{K}'_{\parallel}, \mathbf{k}'_{\parallel}, k'_{ze}, k'_{zh}} |\langle \mathbf{K}'_{\parallel}, \mathbf{k}'_{\parallel}, k'_{ze}, k'_{zh} | H_{ee} | \mathbf{R}_1, \mathbf{R}_2 \rangle|^2 \\
&\quad \times \delta(E_g - 2E_B - [E_{\mathbf{K}'_{\parallel}} + \varepsilon_{\mathbf{k}'_{\parallel}} + \varepsilon_e(k'_{ze}) + \varepsilon_h(k'_{zh})]).
\end{aligned} \tag{5.7}$$

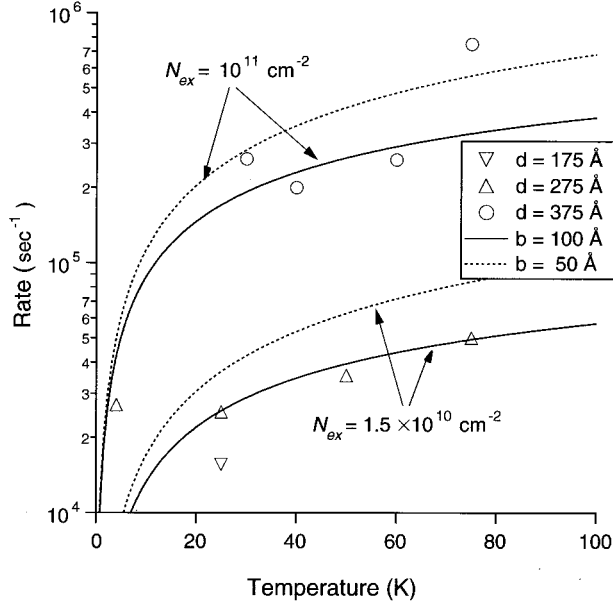


FIG. 8. Over-barrier ionization rate of plane-wave excitons through Auger-like two-exciton processes from a QW with $b=50$ (dotted curve) and 100 \AA (solid curve). Symbols represent TSK's anti-Stokes rate data from samples with $b=100 \text{ \AA}$ (Ref. 3).

The matrix element in Eq. (5.7) can be evaluated from Eq. (5.4) (after expanding the latter to the first order in \mathbf{K}_{\parallel} as before) using the transformation in Eq. (2.6). Because momentum conservation restricts K'_{\parallel} to $K'_{\parallel} \leq 2/\xi$ in Eq. (5.7) and ξ is of the order of b or larger, we neglect $E_{\mathbf{K}'_{\parallel}}$ in the energy δ function. We also approximate $\varepsilon_e(k'_{ze}) + \varepsilon_h(k'_{zh}) = V_0$ as before. The energy δ function then yields $\varepsilon_{\mathbf{k}'_{\parallel}} = E_g - V_0 - 2E_B \equiv E_g^*$.

The rate in Eq. (5.7) is then evaluated without further approximation, yielding

$$W = W_{0,\text{ion}}(\xi) \left[\int_0^{\infty} x e^{-x} B(\sqrt{x}/\xi)^2 dx + \frac{1}{4} \left\{ \int_0^{\infty} \sqrt{x} e^{-x} B(\sqrt{x}/\xi) dx \right\}^2 \right], \quad (5.8)$$

where $W_{0,\text{ion}}(\xi) = (96\pi)^2 N_{\text{ex}} (e^2 D_1 / \kappa)^2 E_B^{*3} / \hbar \xi^2 E_g^{*4}$. This result is identical to Eq. (5.6) if ξ is replaced by ξ_T . Using the parameters in Table I, $N_{\text{ex}} = 5 \times 10^{10} \text{ cm}^{-2}$ and $E_g^* = 1.09 \text{ eV}$ (corresponding to GaAs/Al_{0.3}Ga_{0.7}As), we estimate $W_{0,\text{ion}}(\xi) = 2.67 \times 10^9 \xi^{-2} \text{ sec}^{-1}$ where ξ is in \AA . The calculated rate in Eq. (5.8) is plotted in Fig. 9 as a function of ξ (lower axis) for a 2D exciton density $N_{\text{ex}} = 5 \times 10^{10} \text{ cm}^{-2}$ and is independent of T . The rate is in the range of TSK's data³ which are shown as a function of T in the upper axis.

C. Phonon-assisted exciton transfer

In this section we study one-phonon-assisted Stokes and anti-Stokes rates through dipolar and exchange interactions. The anti-Stokes rate equals $\exp(-\beta\Delta)$ times the Stokes rate.

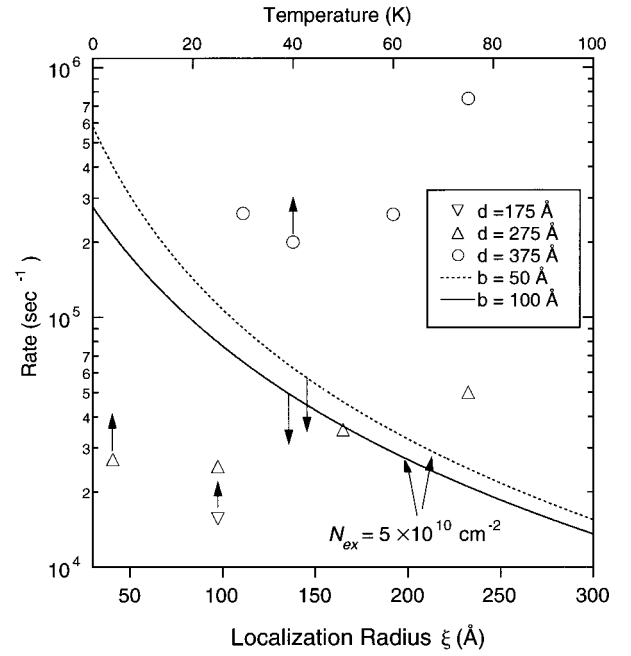


FIG. 9. Temperature-independent over-barrier ionization rate of localized excitons through Auger-like two-exciton processes from 50-\AA (dotted curve) and 100-\AA (solid curve) QW's. Symbols represent TSK's T -dependent anti-Stokes rate data (upper axis) (Ref. 3).

The initial and final states are assumed to be plane-wave exciton states for simplicity. The electron-phonon interaction is given in the j th QW by¹

$$\langle j, \mathbf{K}'_{\parallel} | H_{e\text{-ph}} | j, \mathbf{K}_{\parallel} \rangle = V_{j,\text{sq}} e^{iq_z z_j} \delta_{\mathbf{K}'_{\parallel} - \mathbf{K}_{\parallel}, q_{\parallel}} (b_{\text{sq}} + b_{\text{s}, -q}^{\dagger}), \quad (5.9a)$$

$$V_{j,\text{sq}} = \Xi_{c\mathbf{q}} H_j(\alpha_h \mathbf{q}_{\parallel}, q_z) - \Xi_{v\mathbf{q}} H_j(-\alpha_e \mathbf{q}_{\parallel}, q_z), \quad (5.9b)$$

$$H_j(\mathbf{Q}_{\parallel}, Q_z) = \int d^2 r_{\parallel} \int dz_e \int dz_h \times |F_j(\mathbf{r}_{\parallel}, z_e, z_h)|^2 e^{i(Q_z z_e + \mathbf{Q}_{\parallel} \cdot \mathbf{r}_{\parallel})}. \quad (5.9c)$$

The quantity $V_{j,\text{sq}}$ was introduced in Eq. (4.7) and $\Xi_{c\mathbf{q}}$, $\Xi_{v\mathbf{q}}$ are the electron-phonon coupling constants. Because Δ is larger than the LO phonon energy $\hbar \omega_0 = 36.2 \text{ meV}$, LO phonons play a dominant role. Let $\Xi_{c\mathbf{q}} = \Xi_{v\mathbf{q}} = \Xi_{\text{LOq}}$, where

$$\Xi_{\text{LOq}} = \frac{\Xi_0}{q} = \frac{1}{q} \left(\frac{2\pi \hbar \omega_0 e^2}{\Omega \epsilon'} \right)^{1/2}, \quad \frac{1}{\epsilon'} = \frac{1}{\epsilon_{\infty}} - \frac{1}{\epsilon_s}. \quad (5.10)$$

In the quasi-2D approximation of Eq. (2.7), we find

$$H_j(\mathbf{Q}_{\parallel}, Q_z) = \frac{64 \rho_j(Q_z)}{(Q_{\parallel}^2 a_B^2 + 16)^{3/2}}, \quad \rho_j(Q_z) = \int dz \phi_j(z)^2 e^{iQ_z z}. \quad (5.11)$$

Here, symmetric QW's will be assumed with real $\rho_j(Q_z)$ for simplicity. Inserting Eqs. (5.10) and (5.11) in Eq. (5.9b), we find

$$V_{j,\text{sq}} = V_{\parallel}(q_{\parallel}) \rho_j(q_z) / q, \quad V_{\parallel}(q_{\parallel}) = 64 \Xi_0 \Lambda(q_{\parallel}),$$

$$\Lambda(q_{\parallel}) = \left[\frac{1}{(\alpha_h^2 q_{\parallel}^2 a_B^2 + 16)^{3/2}} - \frac{1}{(\alpha_e^2 q_{\parallel}^2 a_B^2 + 16)^{3/2}} \right], \quad (5.12)$$

where $V_{\parallel}(q_{\parallel})$ is a function of q_{\parallel} only.

The one-phonon-assisted anti-Stokes rate is given after inserting Eqs. (5.12) and (4.7) in Eq. (4.6) by

$$\begin{aligned} W = & \frac{2\pi}{\hbar Z_1 \Delta^2} \sum_{\mathbf{K}'_{\parallel}} e^{-\beta E_{\mathbf{K}'_{\parallel}}} \sum_{\mathbf{K}'_{\parallel}, \mathbf{q}, \pm} [|t_{\mathbf{K}'_{\parallel}}|^2 \rho_1(q_z)^2 + |t_{\mathbf{K}_{\parallel}}|^2 \rho_2(q_z)^2 \\ & - \rho_1(q_z) \rho_2(q_z) (t_{\mathbf{K}'_{\parallel}}^* t_{\mathbf{K}_{\parallel}} e^{iq_z d} + \text{c.c.})] [V_{\parallel}(q_{\parallel}) / q]^2 \\ & \times (n_q + \frac{1}{2} \pm \frac{1}{2}) \delta_{\mathbf{K}'_{\parallel} - \mathbf{K}_{\parallel}, \mathbf{q}_{\parallel}} \delta(E_{\mathbf{K}'_{\parallel}} + \Delta \pm \hbar \omega_0 - E_{\mathbf{K}_{\parallel}}), \end{aligned} \quad (5.13)$$

where \mathbf{q}_{\parallel} is replaced by $-\mathbf{q}_{\parallel}$ for the emission process. We approximate $\rho_j(q_z)^2 = \delta_j^2 / (q_z^2 + \delta_j^2)$ with a correct limit $\rho_j(0)^2 = 1$ and a width $\delta_j \sim \pi / b_j$.¹⁸ We also employ a similar approximation for $\rho_1(q_z) \rho_2(q_z)$ with a width δ' . It turns out that the second and third terms in Eq. (5.13) are negligibly small for $d \gg b_j$.

The dominant term arises from the absorption process (lower sign) in Eq. (5.13). Approximating $n_q = e^{-\beta \hbar \omega_0}$, carrying out the \mathbf{K}_{\parallel} and q_z summations, we obtain

$$\begin{aligned} W = & \frac{e^{-\beta \Delta} \Omega M}{\hbar^3 Z_1 \Delta^2} \left\langle \sum_{\mathbf{K}'_{\parallel}} \frac{1}{2q_{\parallel}} e^{-\beta E_{\mathbf{K}'_{\parallel}}} [|t_{\mathbf{K}'_{\parallel}}|^2 \eta_1(q_{\parallel}) + |t_{\mathbf{K}_{\parallel}}|^2 \eta_2(q_{\parallel}) \right. \\ & \left. - (t_{\mathbf{K}'_{\parallel}}^* t_{\mathbf{K}_{\parallel}} + \text{c.c.}) \eta'(q_{\parallel}) e^{-q_{\parallel} \eta'(q_{\parallel}) d}] V_{\parallel}(q_{\parallel})^2 \right\rangle_{\mathbf{K}_{\parallel}}, \end{aligned} \quad (5.14)$$

where $\mathbf{q}_{\parallel} = \mathbf{K}'_{\parallel} - \mathbf{K}_{\parallel}$ and $E_{\mathbf{K}_{\parallel}} + \hbar \omega_0 = \Delta + E_{\mathbf{K}'_{\parallel}}$. This process is available only to those high-energy excitons in QW1 which can reach the QW2 exciton band with one-phonon absorption. In Eq. (14), $\eta_1(q_{\parallel}) = \eta_2(q_{\parallel}) = \eta'(q_{\parallel}) = 1$ for narrow QW's with $\delta_j \gg q_{\parallel}$. In the opposite limit, $\eta_j(q_{\parallel}) = \delta_j / q_{\parallel}$ and $\eta'(q_{\parallel}) = \delta' / q_{\parallel}$. The analysis has been general so far. For large Δ , we ignore $E_{\mathbf{K}'_{\parallel}} \sim k_B T \ll \Delta - \hbar \omega_0$ at low T 's and approximate $E_{\mathbf{K}_{\parallel}} + \hbar \omega_0 = \Delta + E_{\mathbf{K}'_{\parallel}} \approx \Delta$, $q_{\parallel} \approx K_{\parallel} \approx K'_{\parallel} \equiv [2M(\Delta - \hbar \omega_0) / \hbar^2]^{1/2} = 1/27.8 \text{ \AA}$ in Eq. (5.14).

1. Dipolar phonon-assisted exciton transfer

For the dipolar exchange interaction we use the expression in Eq. (3.5a) for $t_{\mathbf{K}_{\parallel}}$, obtaining from Eq. (5.14)

$$\begin{aligned} W = & \frac{W_{\text{LO}}^{\text{dip}} e^{-\beta \Delta}}{K_{\parallel}^{*2} Z_1} \sum_{\mathbf{K}'_{\parallel}} e^{-\beta E_{\mathbf{K}'_{\parallel}}} [K_{\parallel}^{*2} \eta_1(K_{\parallel}^*) \langle e^{-K'_{\parallel} |R_z|} \rangle^2 \\ & + K_{\parallel}^{*2} \langle e^{-K_{\parallel}^* |R_z|} \rangle^2 \eta_2(K_{\parallel}^*) - K'_{\parallel} K_{\parallel}^* \eta'(K_{\parallel}^*) \langle e^{-K'_{\parallel} |R_z|} \rangle \\ & \times \langle e^{-K_{\parallel}^* |R_z|} \rangle e^{-K_{\parallel}^* \eta'(K_{\parallel}^*) d}], \end{aligned} \quad (5.15a)$$

$$W_{\text{LO}}^{\text{dip}} = \frac{2\pi 64^3 M \omega_0 K_{\parallel}^*}{\hbar^2 \Delta^2 \epsilon'} \left(\frac{e^3 D_1 D_2}{\kappa a_B^2} \right)^2 \Lambda(K_{\parallel}^*)^2. \quad (5.15b)$$

Using $\epsilon'^{-1} = 0.012$ for GaAs (Ref. 19) and Table I, we estimate $W_{\text{LO}}^{\text{dip}} = 3.87 \times 10^8 \text{ sec}^{-1}$. The second and third terms in

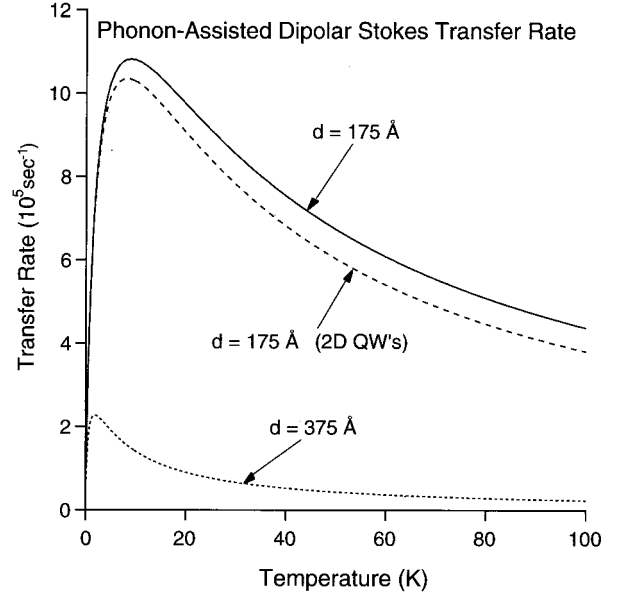


FIG. 10. LO-phonon-assisted dipolar Stokes transfer rate for plane-wave excitons from a 50-Å QW to a 100-Å QW separated by $d = 175$ and 375 Å with $\Delta = 60$ -meV energy mismatch. The dashed curve is for the 2D limit. The anti-Stokes rate is obtained by multiplying the Stokes rate by $\exp(-\beta \Delta)$.

Eq. (5.15) decay exponentially as $\propto \exp(-2K_{\parallel}^* d) = \exp(-d/13.9 \text{ \AA})$ and are negligibly small for large d as confirmed by our numerical analysis. The dominance of the first term means that the excitons prefer to cross the barrier with a small momentum K'_{\parallel} to maximize $|t_{\mathbf{K}'_{\parallel}}|^2 \propto \exp(-2K'_{\parallel} d)$. This is achieved by being scattered inside the initial QW from the initial high-momentum state $\mathbf{K}_{\parallel} = K_{\parallel}^*$ to a low-momentum intermediate state \mathbf{K}'_{\parallel} before crossing the barrier. Using the same argument for the back (i.e., Stokes) transfer from QW2 to QW1, the exciton-phonon scattering occurs in the lower-energy QW1 after crossing the barrier with a small initial momentum K'_{\parallel} .

Retaining only the first term in Eq. (5.15a), carrying out the \mathbf{K}'_{\parallel} summation and employing the approximation given in Eq. (3.7), we find

$$W = W_{\text{LO}}^{\text{dip}} e^{-\beta \Delta} \frac{2k_B T}{E_{K_{\parallel}^*}} \eta_1(K_{\parallel}^*) g(d/\xi_T), \quad (5.16)$$

where $E_{K_{\parallel}^*} = \Delta - \hbar \omega_0$ and the function $g(t)$ was defined in Eq. (3.11a). The one-phonon-assisted Stokes rate due to phonon emission can be derived in a similar way and has the same expression as that in Eqs. (5.15) and (5.16) without the activation factor $e^{-\beta \Delta}$. Comparing with Eq. (3.11), the phonon-assisted Stokes rate $e^{\beta \Delta} W$ has exactly the same T dependence as the dipolar Stokes energy-transfer rate from plane-wave exciton states to free electron-hole pairs. The factor $\eta_1(K_{\parallel}^*)$ indicates (1) that phonon absorption occurs in the initial QW1 and (2) that the rate is a faster rate for a smaller well width as well known.¹⁸ For a numerical estimate we take $\eta_1(K_{\parallel}^*) = 1$ corresponding to the narrow QW limit. Figure 10 displays the T dependence of $e^{\beta \Delta} W$ (i.e., the

Stokes rate) for $d=175$ and 375 Å for $b_1=100$ Å and $b_2=50$ Å.

2. Radiative phonon-assisted exciton transfer

Using a similar expression to that in Eq. (3.18), the photon-exchange coupling between $|1, \mathbf{K}_\parallel\rangle$ and $|2, \mathbf{K}'_\parallel\rangle$ is given by

$$t_{\mathbf{K}_\parallel} = J_{\text{rad}} Q(\mathbf{K}_\parallel, d), \quad J_{\text{rad}} = \frac{16E_g e^2 D_1 D_2}{\hbar \pi c n a_B^2}. \quad (5.17)$$

The quantity $Q(\mathbf{K}_\parallel, d)$ is the same as given in Eq. (3.23) but is different from the specific expression given in Eq. (3.21) where the final state is the free electron-hole state. Using Eq. (3.24) and summing over $\mathbf{D}_1 \parallel \mathbf{D}_2$ and $\mathbf{D}_1 \perp \mathbf{D}_2$, we have the following relationships:

$$\sum_{\parallel, \perp} \langle \|Q(\mathbf{K}_\parallel, d)\|^2 \rangle_{\mathbf{K}_\parallel} = \frac{1}{2} [I_0(x)^2 + |I_1(x)|^2], \quad (5.18a)$$

$$\sum_{\parallel, \perp} \langle Q(\mathbf{K}_\parallel, d) \rangle_{\mathbf{K}_\parallel} = \frac{1}{2} [I_0(x) + I_1(x)], \quad (5.18b)$$

where $x = (K_\parallel d)^2$ and $I_n(x)$ was defined in Eq. (3.26). The quantities on the left-hand sides of Eqs. (5.18) appear in Eq. (5.14) when $t_{\mathbf{K}_\parallel}$ is replaced by $J_{\text{rad}} Q(\mathbf{K}_\parallel, d)$.

The second and third terms in Eq. (5.14) contain terms proportional to $|I_n(x^*)|^2$ and $I_n(x^*)$, respectively, where $x^* = (K_\parallel^* d)^2$. These quantities are negligibly small, indicating that the photon-exchange interaction is small for a large momentum transfer. We therefore retain only the first term in Eq. (5.14). Using Eq. (5.18) and following the same procedure employed for dipolar transition, we find, for $\eta_1(K_\parallel^*) = 1$,

$$W = \frac{W_{\text{LO}}^{\text{rad}} e^{-\beta\Delta}}{2\pi^2} \int_0^\infty dx e^{-x} [I_0(xd^2/\xi_T^2)^2 + |I_1(xd^2/\xi_T^2)|^2],$$

$$W_{\text{LO}}^{\text{rad}} = \frac{64^2 \pi^3 J_{\text{rad}}^2 M \omega_0 e^2}{\hbar^2 \Delta^2 K_\parallel^* \epsilon'} \Lambda(K_\parallel^*). \quad (5.19)$$

The parameters in Table I yield $W_{\text{LO}}^{\text{rad}} = 3.99 \times 10^6 \text{ sec}^{-1}$. The expression $e^{\beta\Delta} W$ in Eq. (5.19) has exactly the same form as that in Eq. (3.29) except for the rate constant $W_{\text{LO}}^{\text{rad}}$. The one-phonon-assisted radiative Stokes transfer rate is displayed in Fig. 11 as a function of T . The rate has the same T and d dependences as the photon-exchange Stokes rate for excitons to transfer into free electron-hole pairs displayed in Figs. 5 and 6, except that it is smaller by a factor $W_{\text{LO}}^{\text{rad}}/W_0 = 1.10 \times 10^{-2}$. Nevertheless, it is about one order of magnitude faster than the phonon-assisted dipolar Stokes rate plotted in Fig. 10. The anti-Stokes rate is smaller by a factor $e^{-\beta\Delta}$.

VI. CONCLUSIONS AND REMARKS

We have studied Stokes and anti-Stokes exciton energy transfer between two asymmetric QW's separated by a wide

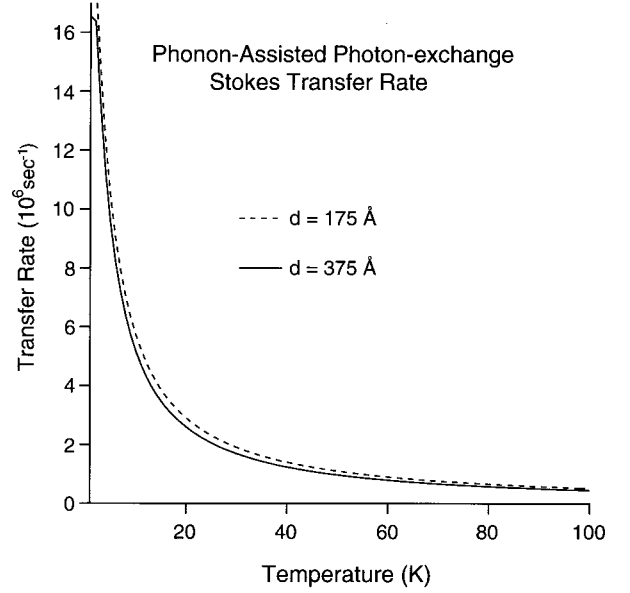


FIG. 11. LO-phonon-assisted photon-exchange Stokes transfer rate for plane-wave excitons from a 50-Å QW to a 100-Å QW separated by $d=175$ and 375 Å with $\Delta=60$ -meV energy mismatch. The anti-Stokes rate is obtained by multiplying the Stokes rate by $\exp(-\beta\Delta)$.

barrier and with a large energy mismatch $\Delta \gg k_B T, E_B$. Several important intrinsic energy-transfer mechanisms have been examined, including dipolar coupling, real and virtual photon-exchange coupling and over-barrier ionization of the excitons via exciton-exciton Auger processes. Phonon-assisted transfer rates were found to be too small to explain the low- T data.

The two most important theoretical predictions of this paper are that the photon-exchange interaction is responsible for the long-distance Stokes energy transfer and that the exciton-exciton Auger processes dominate the anti-Stokes rate at low T 's. In both cases, the rate is insensitive to d if d is smaller than the mean-free paths of the photons for the Stokes transfer and if the over-barrier diffusion of the electrons and holes to the adjacent well is not the rate-limiting process for the anti-Stokes transfer. For the latter, the transfer rate is proportional to the exciton density.

For Stokes energy transfer, the dominant energy transfer occurs through the decay of excitons from the higher-energy QW1 into free electron-hole pairs in the lower-energy QW2. The excess energy is dissipated into the kinetic energy of the electron-hole relative motion. Here, we assume that there are no continuum high-energy localized exciton states in QW2 to enable resonant transfer. However, energy transfer is possible into various low-lying excited bound exciton states but is relatively slow because it requires slow two-step phonon-emission processes to relax the energy as demonstrated in Figs. 10 and 11. The energy-transfer rate through the photon-exchange interaction is much faster than the dipolar transfer rate for $d \geq 80$ Å. In the opposite limit, however, the latter dominates the former. The dominance of the radiative transfer over a large distance d can be understood if we consider transfer from an initial localized exciton state in QW1 to a final localized state in QW2 separated by a distance r . An

analysis similar to that carried out in Sec. III yields a radiative rate between these two states proportional to $1/r^2$.⁵ The total rate can be obtained by summing over the infinite number of final states in the plane of the final QW2, yielding a large rate with very slow dependence on d , decaying logarithmically at large d in contrast with the rapid d^{-4} dependence of the dipolar rate.

The K_{\parallel} component of the interaction between a single dipole of the initial exciton and a plane of dipoles in the final QW has a maximum at $K_{\parallel}=K_{\parallel\text{max}}$ and vanishes at $K_{\parallel}=0$ and $K_{\parallel}d \gg 1$ as shown in Eq. (3.4). This is due to the fact that the net interaction between a point dipole and a line (or sheet) of dipoles vanishes¹⁰ and that the contributions from the individual distant dipoles in QW2 cancel out for $K_{\parallel}d \gg 1$ due to rapid oscillations. As a result, the T dependence of the dipolar rate for plane-wave excitons has a maximum as shown by Figs. 1 and 10. The maximum occurs at the temperature corresponding to the thermal wave number $K_{\parallel\text{max}}$. For localized excitons, the dipolar rate has a maximum at ξ corresponding to $\xi \sim 1/K_{\parallel\text{max}}$.

The K_{\parallel} component of the photon-exchange interaction has a maximum near $K_{\parallel}=K_{\parallel\text{max}}^{\text{ph}}$, saturates at $K_{\parallel}=0$ and vanishes for $K_{\parallel} \gg K_{\parallel\text{max}}^{\text{ph}}$. The maximum occurs when the photon energy becomes comparable to the gap. As a result, the radiative rate is small at $T=0$, quickly reaches a maximum at a very low T , and decays rapidly at higher T 's for plane-wave excitons as shown in Fig. 5. The rate is not plotted below 1 K due to limited graphic resolution. For localized excitons, the maximum rate occurs near $\xi \sim 1/K_{\parallel\text{max}}^{\text{ph}}$ and decays rapidly to zero for $\xi(\sim 1/K_{\parallel}) \rightarrow 0$. The rapid T dependence of the radiative rate displayed in Fig. 5 for plane-wave excitons is not consistent with TSK's data. The rate (shown in Fig. 3) is independent of T for localized excitons if ξ is independent of T . This agrees better with experiment. The excitons may indeed be localized in the initial narrow QW, where the wave functions can be localized even by small layer-thickness fluctuations.

For anti-Stokes transfer through dipolar as well as photon-exchange coupling, we showed in Sec. IV that thermal activation is essential for energy transfer to occur. The single-phonon-assisted rate was calculated using photon-exchange and dipolar coupling, yielding a negligibly small rate at low T 's and an activated T -dependence proportional to $\exp(-\Delta/k_B T)$. In this case, the radiative rate is much faster than the dipolar transfer rate for $d \geq 80 \text{ \AA}$, while the latter dominates the former in the opposite limit. On the other hand, energy transfer through over-barrier ionization of the excitons via Auger-like two-exciton collision processes yielded a significantly larger *nonactivated* rate. This rate is independent of d as long as the diffusion time of the electrons and holes into the adjacent QW is shorter than the ionization time and the electron-hole recombination time. In this process, an exciton is annihilated nonradiatively, imparting its energy to the other exciton, which separates into a free electron and a hole. The basic interaction here is monopole-dipole interaction. This interaction vanishes for $K_{\parallel}=0$ due to the opposite signs of the charge. However, this electron-hole cancellation is avoided for $K_{\parallel} \neq 0$ as seen from Eq. (5.4). As a result, the ionization rate increases as a function of K_{\parallel} , namely with increasing T at low T 's as shown in Fig. 8. At the same time

the rate decreases as a function of $\xi(\sim 1/K_{\parallel})$ as shown in Fig. 9. The rate is independent of T for localized excitons for T -independent ξ . The calculated rate is large enough to explain TSK's data³ (Figs. 8 and 9) if the exciton densities are assumed to be in the range 10^{10} – 10^{11} cm^{-2} . However, the T dependence of the rate predicted by the plane-wave exciton model seems to be more consistent with the data, suggesting that the excitons in the initial *wide* QW may be delocalized due to the relatively smaller effect of the interface-roughness fluctuations.

One existing model proposed for the long-range nature of the energy transfer is by Kim *et al.*²⁰ These authors observed efficient energy transfer over a large distance ranging up to $d=1500 \text{ \AA}$ and attributed it to the percolation of the carriers through hypothetical coherent low-energy GaAs channels connecting the two GaAs QW's through the $\text{Al}_x\text{Ga}_{1-x}\text{As}$ barrier. To support this argument, they studied three different compositions for the barrier, namely the GaAs/AlAs digital alloy, AlAs, and the random $\text{Al}_x\text{Ga}_{1-x}\text{As}$ alloy.^{4,20} The former two structures showed inefficient energy transfer while the latter showed efficient transfer. They concluded that the percolation GaAs channels exist only in a $\text{Al}_x\text{Ga}_{1-x}\text{As}$ barrier. Also, no significant energy transfer was observed between $\text{In}_x\text{Ga}_{1-x}\text{As}/\text{GaAs}$ double QW's. This observation is consistent with the absence of In channels inside the GaAs barrier. According to the predictions of the present paper, however, the observed inefficient energy transfer should follow from short ξ which may be caused by different growth and/or interface conditions. Our anti-Stokes result also relies on efficient diffusion of the carriers above the barrier if it is very wide. The model by Kim *et al.* can be tested by growing a thick layer of GaAs/AlAs digital alloys or AlAs alloys in the middle of a regular (i.e., leaky) $\text{Al}_x\text{Ga}_{1-x}\text{As}$ barrier without disturbing the interfaces of the GaAs QW's. The interfaces of $\text{In}_x\text{Ga}_{1-x}\text{As}/\text{GaAs}$ double QW's are rough due to In clustering, possibly yielding short ξ and thus the observed inefficient radiative transfer in accordance with our theory.²¹

For low-energy localized excitons, ξ is large and the energy depends weakly on ξ . The rate is then a thermally averaged superposition of various ξ . The T dependence of the transfer rate is determined by the ξ dependence of the exciton energy and the distribution of ξ , which are sample-dependent and not well known. The observed T dependence can be used to deduce the information about these parameters. According to our result, a T -independent rate implies a sharp distribution of ξ . There is too much uncertainty in the T and the range dependences of the observed energy-transfer rate for a more satisfactory comparison with our theoretical predictions. A more systematic experimental study is necessary. Our theory serves to provide an order of magnitude estimate for the rates. The anti-Stokes transfer rate through an exciton-exciton Auger process depends linearly on the exciton density. Since this process relies on the over-barrier ionization of the excitons from the lower-energy QW into free electrons and holes, subsequent propagation (diffusion) to the higher-energy QW, and reformation of excitons, an impurity-induced short diffusion length or separation of the electrons and holes by a dc electric field in the barrier will slow down the transfer rate for distant QW's. The electric

field will also decrease the electron-hole overlap in the excitons, affecting the rate.

ACKNOWLEDGMENTS

The author thanks Professor D. S. Kim of Seoul National University for calling his attention to the phenomena discussed in this paper and valuable communications. He also thanks Dr. J. E. Martin for helpful discussions on dipolar interactions and Dr. J. L. Reno for valuable discussions on the growth problems related to GaAs/Al_xGa_{1-x}As structures. We are grateful to Sandia National Laboratories for financial support (U.S. DOE under Contract No. DE-AC04-94AL85000).

APPENDIX A

In this appendix we derive Eq. (3.4). Assuming $\mathbf{D}_1 \parallel \mathbf{x}$, defining $\phi_{\mathbf{K}_\parallel}(\phi_D)$ as the angle between $\mathbf{K}_\parallel(\mathbf{D}_2)$ and the x axis and integrating with respect to the angle between \mathbf{R}_\parallel and \mathbf{K}_\parallel , we find from Eqs. (3.1b) and (3.2)

$$C(\mathbf{K}_\parallel, R_z) = \pi D_1 D_2 \frac{e^2}{\kappa} [(2A_{0,0,3} - 3A_{2,0,5}) \times \cos \phi_D + 3A_{2,2,5} \cos(2\phi_{\mathbf{K}_\parallel} - \phi_D)],$$

$$A_{l,m,n} = \int_0^\infty \frac{r^{l+1} J_m(K_\parallel r)}{(r^2 + R_z^2)^{n/2}} dr, \quad (\text{A1})$$

where $J_m(x)$ is the m th order Bessel function. Inserting¹¹

$$A_{0,0,3} = e^{-K_\parallel R_z / R_z},$$

$$A_{2,0,5} = (2 - K_\parallel R_z) e^{-K_\parallel R_z / 3R_z}, \quad (\text{A2})$$

$$A_{2,2,5} = K_\parallel e^{-K_\parallel R_z / 3}$$

in Eq. (A1), we obtain the result in Eq. (3.4).

APPENDIX B

In this appendix we study the asymptotic behavior of the radiative rate for $d \rightarrow \infty$. Inserting $x = (K_\parallel \xi)^2$, we rewrite Eqs. (3.25) and (3.26) as

$$W = \frac{\xi^2 W_{0,\text{rad}}}{\pi^2} \int_0^\infty dK_\parallel K_\parallel e^{-(K_\parallel \xi)^2} \theta(1/\xi_\Delta^2 - K_\parallel^2) \times [|I_0(K_\parallel^2 d^2)|^2 + |I_1(K_\parallel^2 d^2)|^2], \quad (\text{B1})$$

$$I_n(K_\parallel^2 d^2) = \frac{1}{2} \int_{-\infty}^\infty dk_z e^{ik_z d} \left(\frac{k_z}{k} \right)^{2n} \left\{ \frac{1}{k} + \frac{1}{\xi_g^{-1} - k - i\gamma/d} \right\}, \quad (\text{B2})$$

for localized excitons where $k = (k_\parallel^2 + k_z^2)^{1/2}$ and $k_\parallel = K_\parallel$. For plane-wave excitons, $\xi = \xi_T$ and the step function θ is to be replaced by unity in Eq. (B1). Introducing the identity

$$\frac{1}{(2\pi)^2} \int_{-\infty}^\infty d^2 r_\parallel e^{i\mathbf{r} \cdot (\mathbf{k}_\parallel - \mathbf{K}_\parallel)} = \delta(\mathbf{K}_\parallel - \mathbf{k}_\parallel), \quad (\text{B3})$$

Eq. (B2) is recast into

$$I_n(K_\parallel^2 d^2) = \frac{1}{8\pi^2} \int d^2 r_\parallel e^{-i\mathbf{r}_\parallel \cdot \mathbf{K}_\parallel} \int_{-\infty}^\infty d^3 k e^{i\mathbf{k} \cdot \mathbf{r}} \left(\frac{k_z}{k} \right)^{2n} \times \left\{ \frac{1}{k} + \frac{1}{\xi_g^{-1} - k - i\gamma/d} \right\}, \quad (\text{B4})$$

where $\mathbf{r} = (\mathbf{r}_\parallel, d)$. Carrying out the \mathbf{k} integration in the polar coordinate and also the \mathbf{r}_\parallel integration in the cylindrical coordinate, we find

$$I_n(K_\parallel^2 d^2) = \frac{1}{\xi_g} \int_0^\infty dr_\parallel J_0(K_\parallel r_\parallel) \frac{r_\parallel}{r} \left(\frac{d}{r} \right)^{2n} \int_0^\infty dx \frac{\sin x}{r \xi_g^{-1} - x - i\eta}, \quad (\text{B5})$$

where $\eta = \gamma r/d = r/(\tau\tilde{c})$, $\tau = \hbar/\Gamma$, and the factor $(d/r)^{2n}$ arises from $(k_z/k)^{2n}$ in the limit $d \rightarrow \infty$. The upper limit of the quantity η is the ratio of the sample size to the distance traversed by light during the lifetime and is assumed to be very small (i.e., $\eta \ll 1$). The x integral in Eq. (B5) can be expressed in terms of $\text{ci}(k_g r)$ and $\text{si}(k_g r)$ functions in the limit $\eta \rightarrow 0$, yielding $-\pi e^{-k_g r}$ for $k_g r \rightarrow \infty$, where $k_g = \xi_g^{-1}$.⁵ Therefore, Eq. (B5) can be rewritten in these limits as

$$I_n(K_\parallel^2 d^2) = -\pi k_g \int_0^\infty dr_\parallel J_0(K_\parallel r_\parallel) \frac{r_\parallel}{r} \left(\frac{d}{r} \right)^{2n} e^{-ik_g r}. \quad (\text{B6})$$

When d is much larger than the QW radius, we expand $r = d + r_\parallel^2/2d$. Inserting this result in the exponent of Eq. (B6) and replacing $r = d$ elsewhere, we find¹¹

$$I_n(K_\parallel^2 d^2) = i\pi e^{-ik_g d} e^{iK_\parallel^2 d/2k_g}. \quad (\text{B7})$$

Finally, a d -independent asymptotic rate $W = W_{0,\text{rad}}$ is obtained when Eq. (B7) is inserted in Eq. (B1). Here, the condition $\xi > \xi_\Delta$, is assumed for localized excitons.

In other cases, we change the variable from r_\parallel to r in Eq. (B6), obtaining

$$I_n(K_\parallel^2 d^2) = -\pi k_g \int_0^\infty dr J_0(K_\parallel \sqrt{r^2 - d^2}) \left(\frac{d}{r} \right)^{2n} e^{-ik_g r}. \quad (\text{B8})$$

Hereafter, we study only the contribution from $|I_0|^2$ and show that the rate does not vanish for $d \rightarrow \infty$ but approaches a lower bound slowly. Note also that $d/r \leq 1$ in Eq. (B8) for I_1 and the contribution from $|I_1|^2$ does not alter this conclusion. The integration in Eq. (B8) is given by¹¹

$$I_0(K_\parallel^2 d^2) = \pi i k_g e^{-id\sqrt{k_g^2 - K_\parallel^2}/\sqrt{k_g^2 - K_\parallel^2}}, \quad k_g > K_\parallel$$

$$= -\pi k_g e^{-d\sqrt{K_\parallel^2 - k_g^2}/\sqrt{K_\parallel^2 - k_g^2}}, \quad k_g < K_\parallel. \quad (\text{B9})$$

Inserting this result in Eq. (B1) and going back to the original variable $x = (K_\parallel \xi)^2$ employed in Eqs. (3.25) and (3.26), we find

$$W = \frac{1}{2} \xi^2 k_g^2 W_{0,\text{rad}} \left[\int_0^{(\xi k_g)^2} dx \frac{e^{-x} \theta(\xi^2/\xi_{\Delta'}^2 - x)}{\xi^2 k_g^2 - x + \gamma} + \int_{(\xi k_g)^2}^{\infty} dx \frac{e^{-x} e^{-(2d/\xi)\sqrt{x - \xi^2 k_g^2}} \theta(\xi^2/\xi_{\Delta'}^2 - x)}{x - \xi^2 k_g^2 + \gamma} \right]. \quad (\text{B10})$$

Here, γ accounts for the Lorentzian width and prevents a weak logarithmic divergence at the singularity point x

$= (k_g \xi)^2$ as in Eq. (3.7). The second term in Eq. (B10) vanishes as $(\xi/d)^2/\gamma$ for $d \rightarrow \infty$ and is dropped. The first term can be rewritten in the limit $\gamma \rightarrow 0$ as

$$W = \frac{1}{2} (\xi k_g)^2 W_{0,\text{rad}} e^{-(\xi k_g)^2} \left[\int_0^{(\xi k_g)^2} \frac{e^t - 1}{t} dt + \ln \frac{(\xi k_g)^2}{\gamma} \right]. \quad (\text{B11})$$

Here $\xi > \xi_{\Delta'}$. In view of the fact that $\gamma = d/(\tau \tilde{c})$ ($\ll 1$), the second term decreases logarithmically as a function of d while the first term is independent of d .

-
- ¹T. Takagahara, Phys. Rev. B **31**, 6552 (1985).
²Y. Masumoto, S. Shionoya, and H. Kawaguchi, Phys. Rev. B **29**, 2324 (1984).
³A. Tomita, J. Shah, and R. S. Knox, Phys. Rev. B **53**, 10 793 (1996).
⁴D. S. Kim, H. S. Ko, Y. M. Kim, S. J. Rhee, S. C. Hohng, Y. H. Yee, W. S. Kim, J. C. Woo, H. J. Choi, J. Ihm, D. H. Woo, and K. N. Kang, Solid State Commun. **100**, 231 (1996); D. S. Kim *et al.*, J. Opt. Soc. Am. B **13**, 1210 (1996).
⁵T. Holstein, S. K. Lyo, and R. Orbach, Phys. Rev. B **16**, 934 (1977).
⁶Th. Förster, Ann. Phys. (Leipzig) **2**, 55 (1948).
⁷D. L. Dexter, J. Chem. Phys. **21**, 836 (1953).
⁸R. L. Greene and K. K. Bajaj, Solid State Commun. **45**, 831 (1983).
⁹Y. Shinozuka and M. Matsuura, Phys. Rev. B **28**, 4878 (1983); **29**, 3717(E) (1984).
¹⁰R. Tao and J. M. Sun, Phys. Rev. Lett. **67**, 398 (1991).
¹¹I. S. Gradshteyn and I. M. Ryzhik, *Table of Integrals, Series, and Products* (Academic Press, London, 1980), p. 686.
¹²R. Loudon, *The Quantum Theory of Light* (Clarendon Press, Oxford, 1973), p. 164.
¹³*Semiconductors: Group IV Elements and III-V Compounds*, edited by O. Madelung (Springer-Verlag, Berlin, 1991), p. 101.
¹⁴A. L. Fetter and J. D. Walecka, *Quantum Theory of Many-Particle Systems* (McGraw-Hill, New York, 1971).
¹⁵T. Holstein, Ann. Phys. (N.Y.) **29**, 410 (1964).
¹⁶S. K. Lyo, Phys. Rev. B **61**, 8316 (2000).
¹⁷T. Holstein, S. K. Lyo, and R. Orbach, in *Laser Spectroscopy of Solids*, edited by W. M. Yen and P. M. Selzer (Springer, Berlin, 1981), p. 39.
¹⁸P. J. Price, Ann. Phys. (N.Y.) **133**, 217 (1981).
¹⁹F. C. Brown, in *Polarons and Excitons*, edited by C. G. Kuper and G. D. Whitfield (Plenum Press, New York, 1963), p. 323.
²⁰D. S. Kim, H. S. Ko, Y. M. Kim, S. J. Rhee, S. C. Hohng, Y. H. Yee, W. S. Kim, J. C. Woo, H. J. Choi, J. Ihm, D. H. Woo, and K. N. Kang, Phys. Rev. B **54**, 14 580 (1996).
²¹S. K. Lyo and I. J. Fritz, Phys. Rev. B **46**, 7931 (1992); J. F. Zheng, J. D. Walker, M. B. Salmeron, and E. R. Weber, Phys. Rev. Lett. **72**, 2414 (1994).